

Marginal Price Optimization

A new framework for arbitrage and routing in AMM driven markets

v1.0

Stefan Loesch

`stefan@bancor.network`

Mark Richardson

`mark@bancor.network`

27 January 2025

Abstract

We introduce a new framework for optimal routing and arbitrage in AMM driven markets. This framework improves on the original best-practice convex optimization by restricting the search to the boundary of the optimal space. We can parameterize this boundary using a set of prices, and a potentially very high dimensional optimization problem (2 optimization variables per curve) gets reduced to to a much lower dimensional root finding problem (1 optimization variable per token, irregardless of number of the curves). Our reformulation is similar to the dual problem of a reformulation of the original convex problem. We show our reformulation of the problem is equivalent to the original formulation except in the case of infinitely concentrated liquidity, where we provide a suitable approximation. Our formulation performs far better than the original one in terms of speed – we obtain an improvement of up to 200x against Clarabel, the new CVXPY default solver – and robustness, especially on levered curves.

Contents

List of Figures	4
List of Tables	5
List of Definitions and Theorems	6
1 Introduction	7
1.1 Problem statement	7
1.2 Automated Market Makers	8
1.2.1 Levered liquidity	10
1.2.2 Directional liquidity and fees	12
1.2.3 Limit orders and infinite leverage	13
1.3 Optimization	14
2 Convex Optimization	18
2.1 Setting up the problem	19
2.2 Implementation	23
2.3 Convergence issues	27
3 Marginal price optimization	31
3.1 Definitions and results related to AMMs	32
3.2 Definitions and results related to arbitrage	34
3.3 The Core Equivalence Theorem	39
4 Implementation and convergence	42
4.1 Marginal price optimization on token pairs	43
4.2 General marginal price optimization	47
4.3 Convergence	51
5 Performance comparison	53
5.1 Performance on token pairs	55

5.2	Scaling the number of curves	57
5.3	Mathematical interlude	58
5.4	Scaling the number of tokens	61
6	Conclusion	64
	References	67
A	The Radome Optimization Problem	70
B	The Repatriation Problem	73
C	The Multiple Solutions Problem	76
D	Numerical Methods	78
D.1	Bisection Method	78
D.1.1	Finding roots	78
D.1.2	Finding minima and maxima	80
D.1.3	Convergence	81
D.1.4	Higher dimensions	83
D.2	Newton-Raphson Method	85
D.2.1	Convergence	87
D.2.2	Introducing the learning rate η	89
D.2.3	Higher dimensions	91
E	Explanation of key charts and tables	93
E.1	Curve charts	93
E.2	Trade instruction tables	94
F	Implementation example	96

List of Figures

1.1	Invariance and price curve for an unlevered AMM	10
1.2	Invariance and price curve for a levered AMM	12
1.3	Constraints and target functions	16
1.4	Convolution examples	18
2.1	Single pair arbitrage with three curves	23
2.2	Triangle arbitrage with one curve each	25
2.3	Combined triangle and pair arbitrage including levered curves	26
2.4	Example for curves where convergence fails	28
2.5	Combining two invariant curves	30
4.1	Price response function with no fees	44
4.2	Comparison of price response function with and without fees	45
4.3	Slowdown in convergence as a function of the learning rate	50
4.4	Divergent scenarios for the marginal price optimizer	52
5.1	Calculation time versus number of curves (token pairs)	56
5.2	Calculation time versus number of curves (10 tokens)	57
5.3	Calculation time versus number of tokens (1,000 curves)	62
5.4	Impact of calculating the Jacobian on the overall performance	63
A.1	Example for a radome	71
D.1	Example functions for root search	80
D.2	Bisection progress over time	83
D.3	Attempting multi-dimensional bracketing	84
D.4	Newton-Raphson worked example	86
D.5	Examples of Newton-Raphson with potentially problematic convergence	88
D.6	Impact of the learning rate on the Newton Raphson algorithm	90
E.1	Representation of a single AMM curve with state	93

List of Tables

2.1	Trade instructions (single pair)	24
2.2	Trade instructions (single triangle)	24
2.3	Trade instruction (triangle and pairs)	27
2.4	Trade instructions (levered curves with sentinel)	28
5.1	System configuraton for analysis	54
5.2	Speedup marginal price versus convex (10 tokens)	58
F.1	Token base prices	96
F.2	Curve set with limited arbitrage opportunities	97
F.3	Additional curve providing arbitrage opportunity	97
F.4	Trade instructions with little arbitrage	99
F.5	Trade instructions with little arbitrage, extracting via TKN2	100
F.6	Trade instructions with arbitrage curve	101
F.7	Trade instructions with arbitrage curve, extracting via TKN2	102
F.8	Trade instructions with arbitrage curve, and removing C00	103
F.9	Trade instructions with arbitrage curves only	103

List of Definitions and Theorems

1	Definition (Arbitrage and Routing Problems)	7
2	Proposition (Arbitrage and Routing)	8
3	Definition (Convex Optimization Formulation)	23
4	Definition (Token baskets, Overlap, Larger/Smaller)	32
5	Definition (Direction)	32
6	Definition (Non-improving prices)	32
7	Definition (AMM)	33
8	Definition (Bonding curves and invariant functions)	33
9	Proposition (Convexity)	33
10	Definition (Arbitrage-free)	34
11	Definition (Circularity)	34
12	Proposition (Arbitrage-free unlevered AMMs)	35
13	Proposition (Numeraire)	35
14	Definition (Price vector)	36
15	Theorem (Arbitrage-free AMMs)	37
16	Definition (Price response function)	37
17	Definition (Trade instructions)	38
18	Definition (Marginal Price Formulation)	39
19	Theorem (Core Equivalence)	40
20	Proposition (Existence and uniqueness)	42
21	Observation (Performance comparison)	55
22	Proposition (Jacobian complexity)	60

1 Introduction

Part of Bancor’s product offering is the FastLane Arbitrage bot [15]. When developing this bot, we have developed our own algorithms for solving what we call the “Arbitrage Problem”¹, loosely defined as making risk free money out of a given set of AMMs by trading against them. We started with what we believe was the standard approach at the time, the convex regular convex optimization approach proposed in [6]. This approach worked very well on unlevered curves, but as soon as we applied it to levered curves, we ran into convergence issues that we could not ultimately solve. The main purpose of the FastLane bot was to support the Carbon DeFi protocol [18, 31] and when looking into the problem in more detail, we felt that there were structural reasons why the direct convex optimization approach from [6] would not work well on levered curves. We therefore developed our own algorithm, called the “Marginal Price” algorithm, which solves the same problem, but which is significantly faster and which has more benign convergence properties. It is similar to solving the conjugate convex problem proposed in [12] which was published around the time we put the finishing touches on our arbitrage bot, but it goes somewhat further, and it is more founded in financial than in purely mathematical principles.

1.1 Problem statement

Before we go into the details we will provide key results from [6] that help us to better define the problem space. For clarity of presentation, the references of this section will lead to later sections in the paper. We do not want to hide the forest behind the trees, and whilst the definitions and results referenced are important enough to warrant formal treatment, the concepts are sufficiently widely understood that we are confident that a reader even vaguely familiar with the topic will understand terms like “AMM” without having to look up the formal definition.

Definition 1 (Arbitrage and Routing Problems). *Given a set of AMMs² of a known*

¹See definition 1

²See definition 7

state, the **Arbitrage Problem** is the problem of finding a sequence of trades that will result in a risk-free arbitrage profit³. The **Routing Problem** is the problem of finding a sequence of trades on those AMMs that will result in the highest output (or lowest input) of a "target token" when all other token input and output quantities are fixed.

It turns out that arbitrage and routing are closely related:

Proposition 2 (Arbitrage and Routing). *The Arbitrage Problem is a special case of the Routing Problem where all inputs and outputs except for the target token are fixed at zero.*

Proof. Solving the routing problem where no other tokens go into or out of the system is the definition of an arbitrage according to definition 10. ■

In other words – when solving the routing problem, one is generally also solving the arbitrage problem because arbitrages subsidize the desired exchange, and a pure arbitrage is optimally routing the "null". In this paper, we mostly focus on arbitrage because of our product focus, but transposing the results to routing is generally straightforward.

1.2 Automated Market Makers

In this section, we briefly discuss the concept of *Automated Market Makers* ("AMMs") and their *bonding curves*⁴. Here we focus solely on *constant product curves*, including their levered variety, as they represent all features of interest for our purposes. We note, however, that most results of this paper generalize to other types of curves as well, although it helps when certain quantities can be computed analytically, otherwise interdependent numerical methods can impose additional challenges and performance may be poor. We also note that, in our experience, all relevant curves can be approximated by constant product curves, in segments if need be, which is the approach we take in practice to deal with curves other than constant product curves.

Formally, an AMM is a smart contract that allows the user to trade two or more assets.

³See definition 10

⁴See definition 7 for a formal definition of the concept

The seminal version first introduced by Bancor [21, 22] was a generalized hypersurface $S_{C,\mathbf{r}}$ embedded in R^n , defined by the equation

$$S_{C,\mathbf{r}} = \left\{ \mathbf{x} \mid \prod_{i=1}^n x_i^{r_i} = C \right\} \quad (1.1)$$

where $\mathbf{x} = (x_1, x_2, \dots, x_n) \in R^{n+}$ is the vector of token balances and the $\mathbf{r} \in R^{n+}$ is the associated vector of “reserve weights”. C is a constant.

Equivalently, using the log token balances $\mathbf{z} = \log \mathbf{x}$ where the log function applies on a per-component basis, one can transform the curved hypersurface $S_{C,\mathbf{r}}$ into a hyperplane $P_{C,\mathbf{r}}$ given by the equation

$$P_{C,\mathbf{r}} = \left\{ \mathbf{z} \mid \sum_{i=1}^n z_i r_i = \log C \right\} \quad (1.2)$$

This is the version implemented by Bancor [22] and later by Balancer [28]. The most popular pools on Bancor v1 were all *two-assets / same-weight*. When Uniswap created their first AMM, they froze this as a design principle [2, 3] and they, and many subsequent AMMs including Bancor v2.1/3 and Carbon DeFi, relied on the well known simplified version of the aforementioned constant product bonding curve. This simplified invariant function is defined by the equation

$$x \cdot y = k \quad (1.3)$$

where x and y are the quantities of the two assets, and k is the pool invariant. What this equation signifies is that – ignoring fees – the AMM in question will engage in any trade (ie exchange x for y or vice versa) that keeps the pool invariant k constant. Adding or removing liquidity, including via fees, will of course change k . We can express y as a function of x as $y(x) = k/x$. It is easy to see that the marginal price in units of y per x at a given point (x, y) is given by

$$p_{\text{marg}} \equiv -\frac{dy}{dx} = \frac{k}{x^2} = \frac{y^2}{k} = \frac{y}{x} \quad (1.4)$$

from which immediately follows that, at the marginal price, the value of token holdings in x and y will always be the same, in units of x , or y , or any joint numeraire in which one chooses to express it.

1.2.1 Levered liquidity

The above curves – usually referred to as “*unlevered*” curves for reasons that will become clear in a moment – trade over the entire possible price range. This is nice for symmetry and scale invariance reasons, but it is not particularly efficient in terms of collateral usage, as most tokens in the AMM are held in reserve for price points that, in realistic markets, will never be reached. See figure 1.1 for an illustration of this.

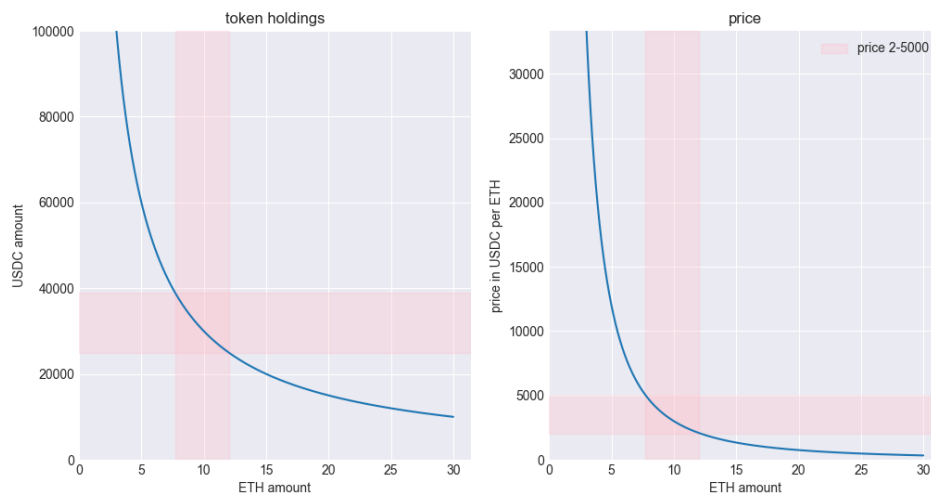


Figure 1.1: *Invariance and price curve for an unlevered AMM.* Invariance (aka bonding) curve (left) and associated price curve (right) for an unlevered AMM; the pink area represents an example for a reasonable trading area, and all collateral outside of it is rarely used.

This is where the concept of virtual token balances and “*amplified*” or “*concentrated*” liquidity curves comes in, first described by Bancor [23] in 2020, and later popularized

by Uniswap [5] in 2021. The idea is simple: we just posited that a significant proportion of the collateral is allocated to price points that will never be reached, so we might as well remove it from the AMM, and if ever the AMM were in a price range where it had to pay out those removed tokens, it would just halt trading until prices returned to the range it was prepared to trade in. To formalize this concept, we introduce virtual token balances⁵ $x_v > 0$ and $y_v > 0$, and with their help we rewrite the invariant equation 1.3 as

$$k = x \cdot y = (x_a + x_v) \cdot (y_a + y_v) \tag{1.5}$$

where $x_a \geq 0$ and $y_a \geq 0$ are the actual token holdings of the AMM. The trading behavior of the AMM is now slightly modified in that – again ignoring fees – the AMM will accept any trade that (1) holds k constant, and importantly (2) maintains x_a and x_b non-negative. What this means in practice is that a levered AMM has two price boundaries – one for $x_a = 0$ and one for $y_a = 0$ – where all the AMM’s collateral is held in the respective other token. An example for a levered curve is shown in figure 1.2 where an amount of 5 ETH or 10,000 USDC (exact mix depends on where we are on the curve) is deployed over a price range of slightly below 1,500 to 3,000 USDC per ETH.

This relatively wide range of a levered curve is typical for Bancor’s original concentrated AMM, and its successor, Carbon DeFi. However, architecture and design decisions made for the Uniswap v3 AMM mandate a much thinner range: the minimum tick size depends on the fee tier, but the width of a single Uniswap v3 curve was initially between 10-200 basis points. What is usually referred to as “the” Uniswap v3 curve is actually a collection of independent curves that are located adjacent to each other, each of which have their own liquidity holdings.

⁵Some authors disagree on what exactly is being referred to as *virtual* token balance, the quantity x_v or the sum $x_v + x_a$; herein, we use the former, but in any case it should always be clear from the context

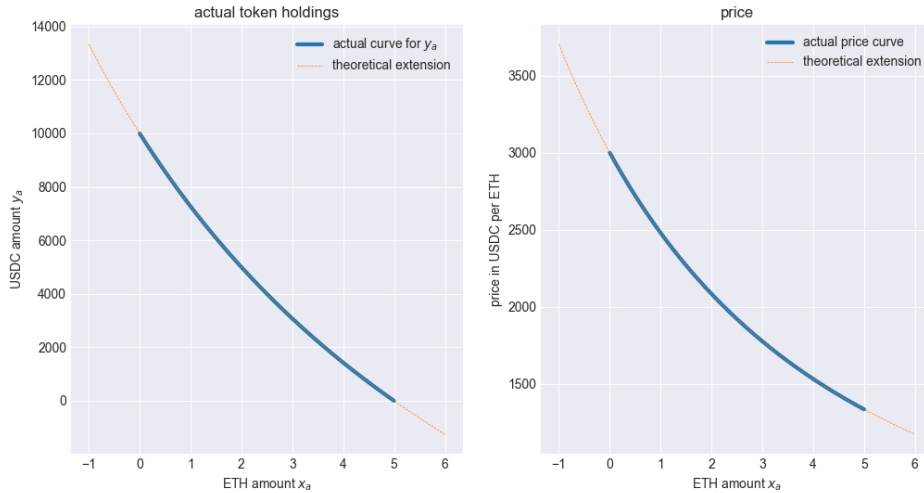


Figure 1.2: *Invariance and price curve for a levered AMM*. Invariance (aka bonding) curve (left) and price curve (right) for a levered AMM; only the area in solid blue corresponds to actual liquidity held by the AMM. The thin curve extending it depicts where the associated unlevered AMM would trade.

1.2.2 Directional liquidity and fees

Directional liquidity, also referred to as “*asymmetric liquidity*”, is a concept that has been formally introduced by Bancor with its Carbon DeFi product in 2022 [34, 31]. It means that specific curves only ever trade in one direction, and that if one wants to offer a two-way market, one has to explicitly specify two curves for that. Technically, a directional curve in Carbon is implemented as a levered curve according to equation 1.5 with the stipulation that one of x_a, y_a is always kept at zero. In other words, whilst in a non-directional AMM, tokens that trade into the AMM are added to the actual token balances, x_a, y_a respectively, to replace those that have been traded out, in a directional AMM the tokens that are traded in are added to the retained token balances, x_r, y_r respectively.

For those retained balances the Carbon AMM design then offers two choices:

- they are off-curve and inactive, and their only future use is that they can be withdrawn by the owner of the curve, or

- they are automatically placed onto another curve that trades into the opposite direction, with parameters independent of that of the first curve.

In a Carbon DeFi context, buy and sell curves are typically non-overlapping. For example, a curve may buy ETH against USDC between 2,500-2,600 and sell it between 2,900-3,000. However – *overlapping strategies* are also possible where the parameters are chosen such that the price of the buy and sell curve move in unison, and that collateral that moved from the buy to the sell curve is offered back to the market at only a slightly higher price.

It is an important insight – and the reason why we wrote “formally” introduced above – that functionally, overlapping strategies are not different from non-directional curves with fees. For example, a curve that buys and sells the marginal ETH at 3,000 USDC with a 1% fee is functionally equivalent to one curve that buys ETH at 2,970 USDC and another that sells it at 3,030 USDC, and collateral moves from one curve to the other upon trading.

Fees will become very important further down this paper because they actually lead to curve scenarios that are numerically not particularly well behaved. We will get into the details of this further ahead, but the key reason is that in the presence of fees there are “holes” in the curve where it does not exist. For example the curve above would not trade at all for prices between 2,970 and 3,030 USDC, and any algorithm that performs a local analysis at this price point risks failing.

1.2.3 Limit orders and infinite leverage

Bancor, via its Carbon DeFi product, also introduced the concept of limit orders into the AMM space, where the entire liquidity of a curve is placed at a single price point. Formally, this can be considered as the limit $x_\nu, y_\nu \rightarrow \infty$ in equation 1.5 and in our preprint [33]. In practical calculations this of course does not help us much as we cannot deal numerically with numbers that are infinite. The Carbon DeFi implementation gets around this by reparametrizing the problem in terms of $B = \sqrt{p_{\min}}$ and $A =$

$\sqrt{p_{\max}} - \sqrt{p_{\min}}$, where p_{\min} and p_{\max} are the marginal prices at the boundaries, which allows setting $A = 0$ for limit orders. However, in our implementation of the arbitrage bot (productized as Bancor’s “*ArbFastLane protocol*”), and throughout this paper, we do not allow for $A = 0$ as this would lead to numerical instabilities in the calculations. Instead, we impute a minimum value for A that is big enough for numerical stability, and that is then being corrected in a transaction fine tuning process once arbitrage opportunities have been identified.

1.3 Optimization

Before we dive further into the issue at hand, we want to generally discuss optimization problems and start building intuition on how they work, and how they can be solved⁶. Generally, an optimization problem has (1) a target function, and (2) one or more constraints. We then are looking to maximize or minimize the target function while satisfying the constraints. The constraints can be equality constraints, inequality constraints, or both. Equality vs inequality does not usually make a difference as the solution to a sufficiently well conditioned optimization problem is found on the boundary of the feasible region. Constraints can be of two kinds which we call “*(multi-)linear*” or “*explicit*”, respectively. The former consist of *multiple* linear inequalities and all of them must be satisfied, leading to a non-differentiable hypersurface where the non-differentiable regions are the boundaries on which the active constraint switches. What we call explicit constraints are constraints that can be written in the form $f(x) = 0$ for some function f . We call an explicit constraint *smooth* if it can be written using a single smooth constraint function f . Note that the two forms of constraints are often interchangeable. For example, every multi-linear constraint can be converted into an explicit constraint using a piecewise-linear function f , but depending on the exact use case one or the other may be easier to deal with. Linear constraints have the advantage that the resulting set will be convex. Also, in higher dimensions it is usually hard to formulate an explicit constraint function matching multiple linear constraints.

⁶Please also refer to appendix D for a discussion of the numerical methods we use

In figure 1.3 on the left hand panel, we have drawn an optimization problem in one dimension where the blue and orange lines represent the constraints, linear and smooth respectively, and the grey lines represent level sets of the target function. We have also drawn the derivative of the constraint and target functions in the same figure, on the right hand panel.

In one dimension, this problem is easy to solve: the point where the target function is optimized in the smooth case is where the level set is tangent to the constraint. In other words: we look for the point where the derivative of the target function equals the derivative of the constraint, which in this case happens slightly below $x = 1$. For the linear case, we encounter another well known result of optimization theory which is that the solution to the optimization problem is usually found on the lowest-dimension boundary, which in this case are the points where the different constraints meet. In this case the solution is exactly at $x = 1$. Note that whilst this is not technically a point where the constraint is tangent to the target function, the derivative of the constraint flips from above to below the derivative of the target function. If we would smooth the corners of the constraint function – say by folding with a C^∞ kernel – we would find that the derivatives would again meet very closely to $x = 1$, the exact point depending on the kernel used.

Ultimately, as we will see in what follows, this problem shows the essence of what we are aiming to do in this paper, except that the problem we are solving is higher dimensional, and the functions we consider are more complex, so that we do have to rely on numerical methods to find the solution. Specifically, the target function is the profit made, or rather the outflow in the target token chosen to collect the profit. The constraints are given by the AMM curves that form the market, plus the “self-financing-constraint” that all token flows must be accounted for (ie that there is no net token leakage in or out other than the one explicitly accounted for). In the pure arbitrage case, this constraint is simply that, on a net basis, all flows in tokens other than that of the target token are zero. We mention en-passant that for routing applications one can use other constraints, eg “*there is a flow*

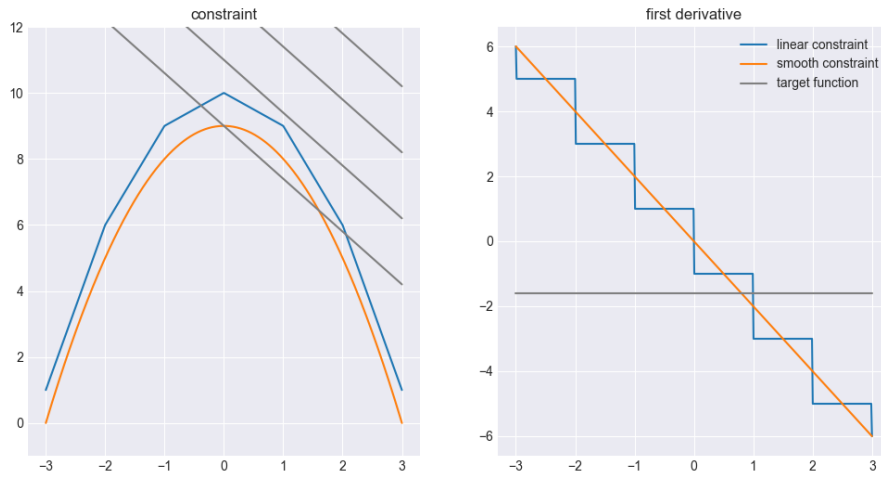


Figure 1.3: *Constraints and target functions.* The left panel depicts a smooth constraint (blue) and a piecewise-linear one (orange) as well as the level areas of a linear target function (grey). The right panel shows the respective derivatives, showing that at the optimal point, the derivative of the target function equals the derivative of the constraint.

of 1,000 USDC into the system” (or “1,000 USDC and 3,000 DAI”), and answering the question “what is the maximum amount of ETH that can be extracted and how?” is the answer to the optimal routing problem. However, whilst the routing application is interesting and not particularly hard to execute once the arbitrage application settled, it is not the focus of this paper.

As shown by Angeris et al in reference [6], this problem is a convex optimization problem, and as we will see, we will run into similar problems that generic convex solvers run into, which is that smooth problems and linear problems often require different algorithms. Specifically, smooth problems are often solved using gradient descent methods, whilst linear problems are often solved using simplex methods, the latter essentially jumping between the vertices of the feasible region. The reason why we run into those problems is that we sometimes have a smooth problem, sometimes a linear problem, and most of the time a problem that is dominated by one of the two aspects, although it is hard to

predict which one in advance⁷. Specifically:

1. A market that only consists of unlevered curves is a smooth problem.
2. A market that only consists of limit order curves (eg, Carbon curves with width zero) is a linear problem
3. Levered curves are a mix of the two, depending on their width, or rather: how fast the liquidity changes at different points in the curve (“ticks” in Uniswap v3 parlance).

We can think of the third case above as a “smoothed” problem where the width of the curves corresponds to the smoothing kernel used. We briefly explain the concept of smoothing kernels in figure 1.4. In its left panel, we have drawn a few Gaussian kernels with different width parameter λ . They satisfy the equation

$$\kappa_\lambda(x) = \sqrt{\frac{\lambda}{\pi}} e^{-\lambda x^2} \quad (1.6)$$

When we calculate the convolution of the kernel κ with the target function f (here, the constraint function), we get

$$f_\kappa(x) = (\kappa * f)(x) = \int \kappa(x - y) f(y) dy \quad (1.7)$$

Note that, as mentioned above, because the kernel κ is C^∞ , the convolution f_κ is also C^∞ which we can easily show by pulling the differentiation operator ∂_x inside the integral so that we get $f'_\kappa(x) = (f * \kappa')(x)$ where the f' and κ' respectively denote the derivative with respect to the variable x . The convolution of a piecewise-linear function with a C^∞ kernel, together with the kernel examples, is shown in figure 1.4.

We do not use convolution explicitly in our algorithms but we enforce a minimum width for limit orders which has the same effect: if we convert a *buy-at-1,000* limit order to

⁷In this context see appendix A for the *radome optimization problem* that provides a geometric example for a problem exposing similar issues

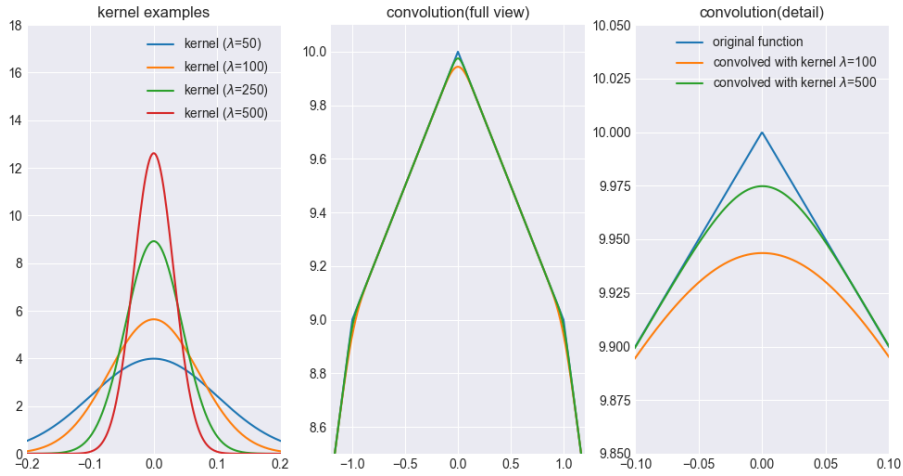


Figure 1.4: *Convolution examples*. The left panel shows a number of Gaussian C^∞ kernels of different widths. The other panels show a zoomed out (middle) and detailed view of a piecewise linear function (blue) and its convolution with two kernels of different widths (orange and green) which is a C^∞ function.

buy-from-990-to-1,001 then this is akin to a convolution of the constraint function with a kernel of about unity width.

2 Convex Optimization

The marginal price optimization algorithm for arbitrage and routing, described in section 3, is the core of this paper. It is closely related to the convex optimization algorithm described in [6, 7, 12] that we were previously using. As described in section 2.3, when we applied that algorithm for Bancor’s ArbFastLane product [15] to markets containing important segments with levered curves we ran into unsurmountable convergence issues.

We will not go into the details of convex optimization here – the aforementioned references are excellent resources for that. However, a description of the convex optimization setup is important for setting the scene and context in which our core theorem of this paper, the *core equivalence theorem* 19, establishing the equivalence between our marginal price optimization algorithm and the previously known convex optimization algorithm.

This will happen in the next subsection 2.1, and in the following section 2.2 we will discuss implementation and results of the convex optimization algorithm on unlevered curves where it works extremely well. In the last subsection 2.3 we will finally discuss convergence issues, providing a specific example of a problematic case.

2.1 Setting up the problem

We will here briefly outline the methodology that we used as a basis for our implementation. It closely follows [6] so interested readers are encouraged to read both papers in conjunction.

For setting up a convex optimization problem, we need to define the *optimization variables*, the *target function* and a set of *constraints*. The target function is the function that we want to optimize, and the constraints are the conditions that the variables must satisfy.

Optimization Variables. We are operating in the context of a linked set of DEXes, and the natural variables are the token balances of all those DEXes, as those fully define the state of the system that we are interested in. For ease of notation and WLOG we only consider DEXes that operate on token pairs, but it should be noted that conceptually, multi-token exchanges work the same way, but the notation gets significantly heavier.

We assume that we have M DEXes indexed by $\nu = 0 \dots M - 1$. Those DEXes have $2M$ token balances x_0, \dots, x_{2M-1} where we simply assume that adjacent balances belong to a given DEX, ie $x_{2\nu}$ and $x_{2\nu+1}$ are the token balances of DEX ν . We use $\alpha = 0 \dots 2M - 1$ as index for the balances.

Positivity Constraints. The basic constraint is that all token balances must be non-negative, ie

$$\forall \alpha = 0 \dots 2M - 1 : \quad x_\alpha \geq 0 \tag{2.1}$$

For unlevered curves, those constraints can often be omitted, because they are not binding. However, they are relevant in the case of levered AMMs where those balances are virtual balances according to equation 1.5. Also, many solvers operate more efficiently if positivity constraints are explicitly stated.

Curve Constraints (unlevered). The token balances satisfy the following curve constraints or *curve (in)equalities*

$$\forall \nu = 0 \dots M - 1 : \quad x_{2\nu} \cdot x_{2\nu+1} \leq \bar{x}_{2\nu} \cdot \bar{x}_{2\nu+1} \equiv \bar{k}_\nu \quad (2.2)$$

The barred quantities \bar{x}_α are the initial values of the token balances, so those are not optimization variables, but parameters of the problem. The redundant terms \bar{k}_α are only shown to link back to the curve equation 1.3.

Curve Constraints (levered). When using levered curves we recreate the step from equation 1.3 to equation 1.5 and we rewrite equation 2.2 as

$$\forall \nu : \quad (x_{2\nu} + \bar{x}_{2\nu}^0) \cdot (x_{2\nu+1} + \bar{x}_{2\nu+1}^0) \leq (\bar{x}_{2\nu} + \bar{x}_{2\nu}^0) \cdot (\bar{x}_{2\nu+1} + \bar{x}_{2\nu+1}^0) \quad (2.3)$$

This equation states that the current state of the AMM is adjusted by the virtual base balances \bar{x}_α^0 , which are additional, constant, parameters of the problem.

Technically, the constraints in 1.3 and 1.5 should be equalities, but as shown in [6], inequalities are required to make the problem convex. However, the solution to the optimization problem will be found on the boundary, so any solution will actually satisfy the equality constraints as opposed to the inequality ones.

Token Flows. Up to here we have treated all token balances as independent variables, which misses one very important piece of information, notably what type of tokens they are (eg WETH, USDC etc). This information is provided in the form of *self-financing constraints* which ensure that the sum of the balances of the same token across all DEXes

is constant, with the exception of the *target token* which is the token in which the profits are being extracted (see below). In other words: those constraints ensure the we do not move tokens other than the target token in or out of the system.

We assume here that we have $N + 1$ tokens indexed by $i = 0 \dots N$ and that token $i = 0$ is the *target token*. We want to define the *token flows* ϕ_i as changes in token balances of token i before and after the optimization. In order to do that, we define the *token matrix* \mathbf{T} as

$$\mathbf{T} = (T_{i\alpha}), \quad T_{i\alpha} = 1 \text{ if } (x_\alpha \text{ of type } i) \text{ else } 0 \quad (2.4)$$

In other words, $T_{i\alpha}$ is the indicator function for the token associated with the DEX balance x_α being of token type i .

Using this token matrix, we can now express the *token balance function* $\mathbf{B} : R^{2N} \rightarrow R^{N+1}$ as a function from the state space into the “balance space”, associating each state $x = (x_\alpha)$ a balance vector $\mathbf{B}(x) = (B_i(x))$ where $B_i(x)$ is the sum of the token balances of token i across all DEXes. Using the token matrix we can write this in matrix form as

$$\mathbf{B}(x) = \mathbf{T}x \quad (2.5)$$

or, broken down into its components, as

$$B_i(x) = \sum_{\alpha=0}^{2M-1} T_{i\alpha}x_\alpha \quad (2.6)$$

This finally allows us to define the aforementioned *token flow function* $\phi : R^{2N} \rightarrow R^{N+1}$ as the difference between the token balance function after optimization $\phi(x)$ and the initial token balance function $B(\bar{x})$ as

$$\phi(x) = B(x) - B(\bar{x}) \tag{2.7}$$

The convention here is that outflows from the DEX system are negative, and inflows to the DEX system are positive.

Self Financing Constraints. The self-financing constraints we use for arbitrage calculation is that, other than for the target token $i = 0$, the flow must be zero, yielding

$$\forall i = 1 \dots N : \quad \phi_i = 0 \tag{2.8}$$

Note that we start at $i = 1$ because we excluded the target token from the token flow calculation. Whilst the optimal routing problem is out of scope for this paper, we note that if we are interested in routing instead of arbitrage, the above equation becomes

$$\forall i = 1 \dots N : \quad \phi_i = w_i \tag{2.9}$$

where $\mathbf{w} = (0, w_1, \dots, w_M)$ is the vector of desired flows to route into or out of token 0.

Target Function. Last but not least we need to define our target function (ie the function that we want the optimizer to minimize or maximize). In our case, we want to maximize our profit, and our profit is the outflow of target token $\nu = 0$ from the system, which in our conventions is a negative number. Therefore our optimizer target is

$$\text{target} = \min \phi_0(x) \tag{2.10}$$

and the optimizer should minimize the negative number $\phi_0(x)$ ⁸.

We can tie all those definitions together in the following definition. As mentioned above,

⁸This definition is WLOG in that we could optimize for any other token but token 0, but this would unnecessarily complicated the formulas.

the proof that this is a *convex* optimization problem is given in [6].

Definition 3 (Convex Optimization Formulation). *The "Convex Optimization Formulation of the Arbitrage Problem" is the convex optimization problem with the target function from equation 2.10 which is subject to the positivity constraints in equation 2.1, the self-financing constraints in 2.8, and the curve constraints either in their unlevered form in 2.2 or their levered form in 2.3, or a combination thereof.*

2.2 Implementation

An example implementation of this algorithm is given in [6] appendix B, and we refer the interested reader to that reference for a worked example. Like in that example, when we started working on the ArbFastLane arbitrage bot [15, 16] we implemented the algorithm in Python using the CVXPY library [8, 9, 13].

See appendix E for a detailed explanation of our charts and tables.

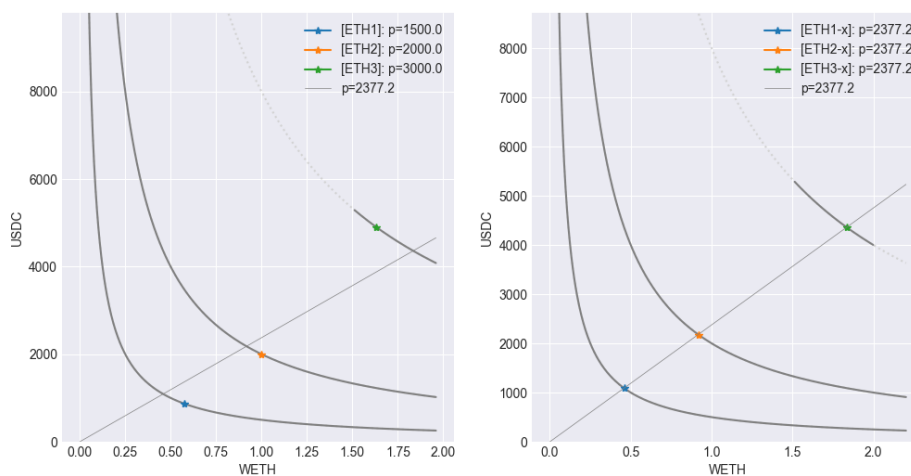


Figure 2.1: *Single pair arbitrage with three curves.* The left panel shows three curves of the same pair WETH/USDC, all at different prices (the stars are not aligned). The right panel shows the same curve after the arbitrage process, where all three stars are on the same line from the origin, at a price of 2377.

In the pair arbitrage figure 2.1 we show three curves, all operating in the same pair

	WETH	USDC
PRICE	2,377.2	1.0
ETH1	-0.119	224.201
ETH2	-0.083	180.452
ETH3	0.201	-538.075
AMMIn	0.201	404.653
AMMOut	-0.201	-538.075
TOTAL NET	-0.000	-133.423

Table 2.1: Trade instructions (single pair)

WETH/USDC. As shown in the left panel, initially they are at different prices. The result after running the optimization algorithm is shown in the right panel, where all three curves are now at the same price of 2377. Therefore, all three stars indicating the current state of the curves are on the same straight line through the origin. The associated trade instructions are in table 2.1.

	WETH	WBTC	USDC
PRICE	2,624.8	23,673.0	1.0
ETH1	-0.141		279.578
BTC1		0.016	-380.457
BE1	0.141	-0.016	
AMMIn	0.141	0.016	279.578
AMMOut	-0.141	-0.016	-380.457
TOTAL NET	-0.000	-0.000	-100.879

Table 2.2: Trade instructions (single triangle)

We then look at a simple triangular arbitrage, where we add WBTC as a third token, and where we have curves for each of the three constituent pairs, as shown in the left column of charts in figure 2.2. Note that, if we multiply the first two prices, we do not get the third one, meaning that there is a circular arbitrage opportunity. After the arbitrage process, the stars indicating the state of the AMM changed their location, and the product of the first two prices equals the last one, therefore no further arbitrage opportunities are left. The associated trade instructions are in table 2.2.

Finally, in figure 2.3 in the left column, we look at a triangular scenario with multiple curves per pair, presenting both pairwise arbitrage opportunities (the stars are not on the

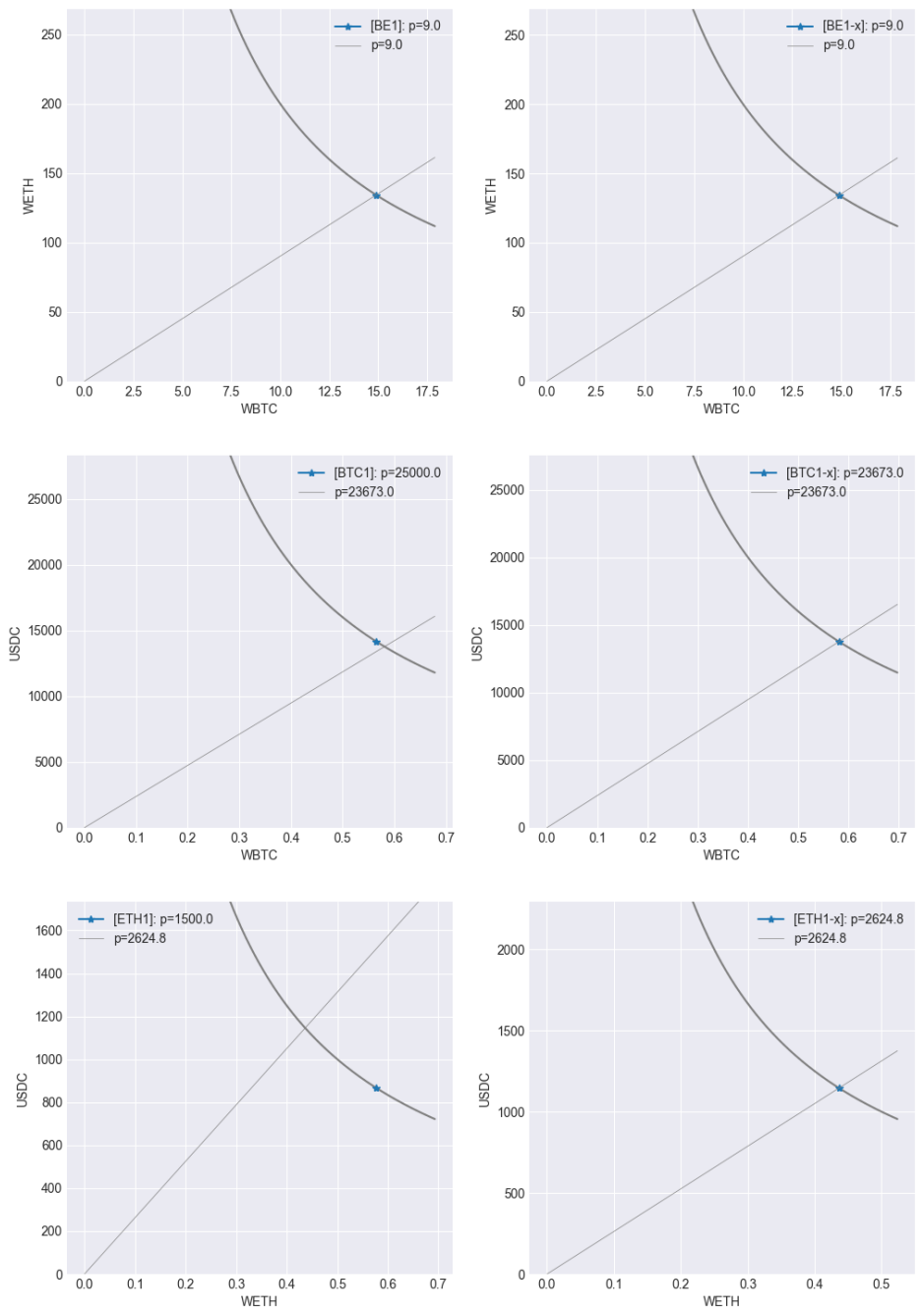


Figure 2.2: *Triangle arbitrage with one curve each.* The three charts on the left represent curves in the triangle WETH/USDC/WBTC, at price points that allow a circular arbitrage. The right panel shows the same curves after the arbitrage process, where the stars are aligned so no circular arbitrage is possible.

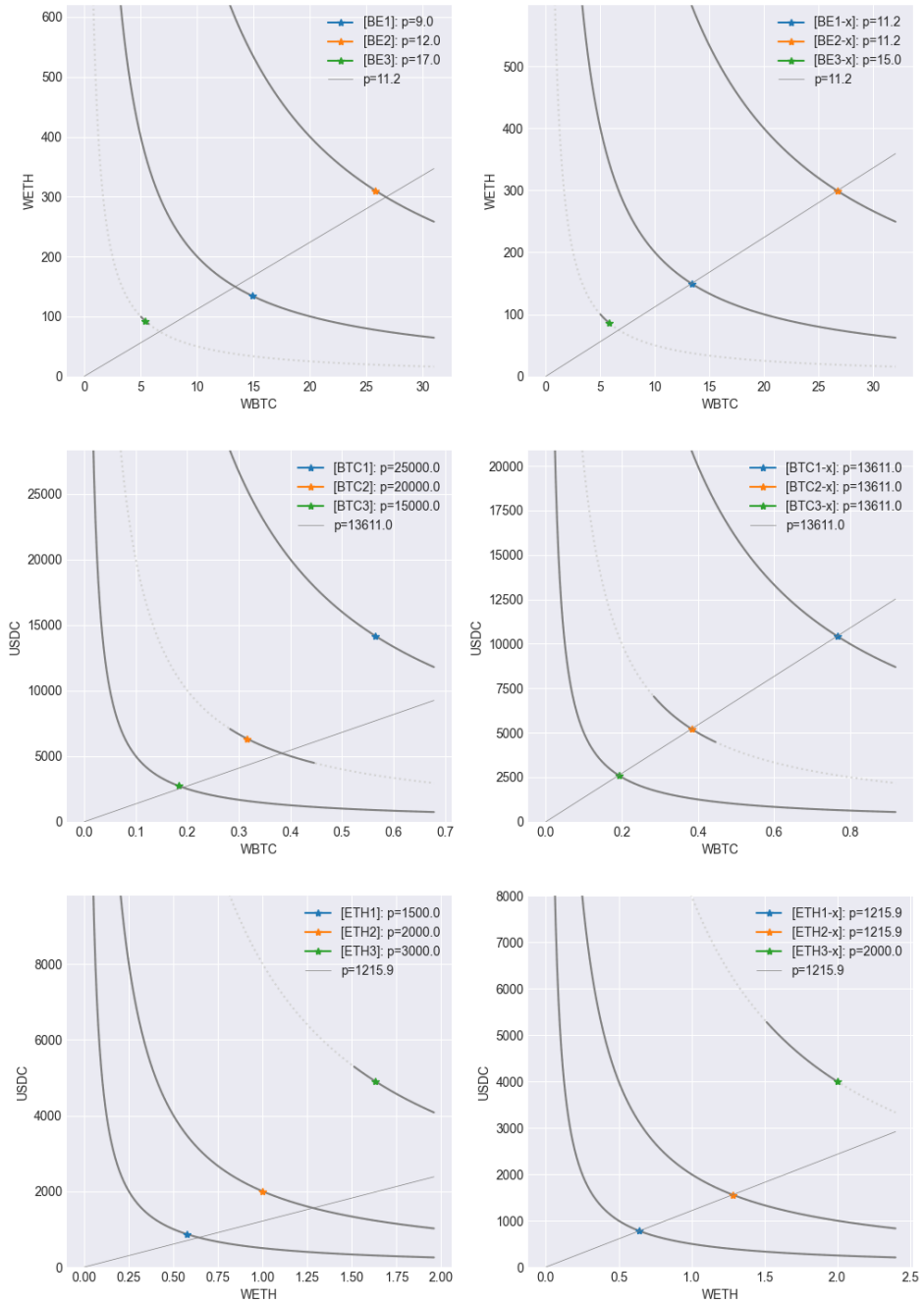


Figure 2.3: *Combined triangle and pair arbitrage including levered curves.* The curves on the left represent a market where both pair and triangular arbitrage is possible, the former being visible by the fact that the stars are not aligned. The right panel shows the same curves after the arbitrage process, where all stars are either aligned, or at the correct boundary in case of levered curves outside of their range.

	WETH	WBTC	USDC
PRICE	1,215.9	13,611.0	1.0
ETH1	0.064		-86.315
ETH2	0.283		-440.579
ETH3	0.367		-898.979
BTC1		0.201	-3,707.206
BTC2		0.067	-1,107.091
BTC3		0.009	-129.880
BE1	15.463	-1.541	
BE2	-10.584	0.913	
BE3	-5.593	0.350	
AMMIn	16.177	1.541	0.000
AMMOut	-16.177	-1.541	-6,370.051
TOTAL NET	-0.000	-0.000	-6,370.051

Table 2.3: Trade instruction (triangle and pairs)

same straight line from the origin) and triangular ones (the products of the prices once aligned do not match). In the right column of figure 2.3 we present the post arbitrage scenario, and the associated instructions are in table 2.3. Note that the stars indicating the current states of the AMMs are not all aligned: those on the unlevered curves are, but some of the levered curves are stuck at the boundary closest to the relevant price point. Again, the circular price equation is satisfied but only for the aligned prices corresponding to interior points on the curves.

2.3 Convergence issues

In scenarios like the one above, that are dominated by unlevered or sufficiently wide levered curves, we have found that the algorithm converged well. It however ran into issues in scenarios dominated by narrow levered curves. We have shown a simple example for those types of curves in figure 2.4. On the left hand panel we see two levered curves that are in the money against each other: one curve buys WETH at around 2,500, one sells it at around 1,500, with an overall profit opportunity of around 17 USDC. None of our convex solvers would converge with that problem. However, if we add a reasonably sized unlevered *sentinel curve* – the unlevered curve added in the right panel of figure 2.4 – then convergence succeeds, even though the sentinel curve does not in this case

participate in the arbitrage trade, proving that convergence on this problem should be possible⁹ even without the sentinel curve. The associated trade instructions are in table 2.4.

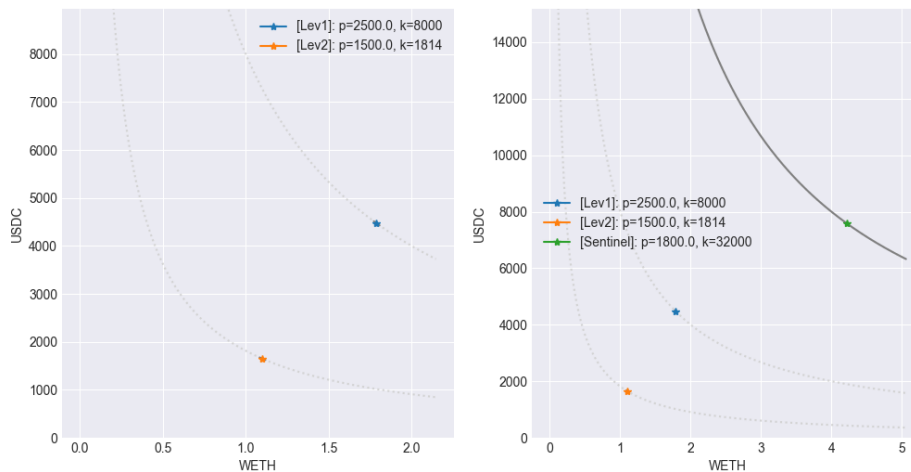


Figure 2.4: *Example for curves where convergence fails.* The left hand panel shows two levered curves that are in the money against each other and where the algorithm fails. Adding a sufficiently large sentinel curve (right panel) allows the algorithm to converge, with no trading on the sentinel curve.

	WETH	USDC
PRICE	1,800.2	1.0
Sentinel	-0.000	0.502
Lev1	0.018	-44.947
Lev2	-0.018	27.268
AMMIn	0.018	27.769
AMMOut	-0.018	-44.947
TOTAL NET	-0.000	-17.178

Table 2.4: Trade instructions (levered curves with sentinel)

We have not formally shown this, but we suspect that the issues we see are related to the phenomenon we have hinted at in a very simple case in section 1.3: there is a difference

⁹Looking ahead, the marginal price optimizer that is subject of this paper and that we describe in section 3, however, does converge well in this case; failure of the convex algorithm to converge on curves that we were interested in, rather than the improvement in speed was the original reason why we investigated the development of a new algorithm to replace convex optimization

between how to deal with smooth constraints and general linear constraints. Specifically, in the smooth case, a gradient descent method can be used, or some other numeric solver which allows us to solve for the condition that *the gradient of the constraint equals the gradient of the target function*. For piecewise-linear constraints this no longer works, and we need to use a method like the simplex method [29] that jumps between the vertices of the feasible region. In practice, our constraints are piecewise smooth, meaning sometimes we get interior solutions like in the smooth case, and sometimes we get corner solutions like in the linear case¹⁰. We have not found a convex solver that that can be relied upon to consistently perform well¹¹ under those circumstances.

Financially, the smooth vs corner solution cases are easily understood: an interior solution is a situation where – in the region of interest – the curves provide liquidity in both directions, and no abrupt changes in liquidity occur when moving prices. On the other hand, a solution where levered curves trade, but end up at their boundary is a corner solution. An example for an interior solution is any collection of Uniswap v2 pools, or Uniswap v3 pools with sufficient liquidity in and around the current tick that the trades do not fully empty the current-tick pool in one direction. The archetypical example for a corner solution are Carbon DeFi limit orders that are in the money against each other (eg one curve selling 1 TKN at 100 USDC and another curve buying it at 105 USDC). This is a highly non-smooth problem where no gradient method will work. However, simplex methods usually work just fine.

The specific issue for using a convex optimization algorithm in a production environment is that it is very hard to predict which case we are in before we have actually solved it. We go back to the “*sell TKN at 100 USDC, buy it at 105*” example. If both curves are sufficiently narrow, the transaction will bring at least one of the two curves to its boundary, meaning that after the transaction at least one of the curves is either completely empty or completely full. However, if the curves are wide enough, then

¹⁰See appendix A for a description of the *radome optimization problem* that is a very similar geometric problem

¹¹We note that because we developed the marginal price optimization algorithm before the publication of [12] we never tried the conjugate algorithm developed there

this does not happen. Instead, the transaction will stop at the point where the marginal prices on the two curves coincide, and, therefore, where every additional dollar transacted would have a negative marginal contribution to the transaction profit.

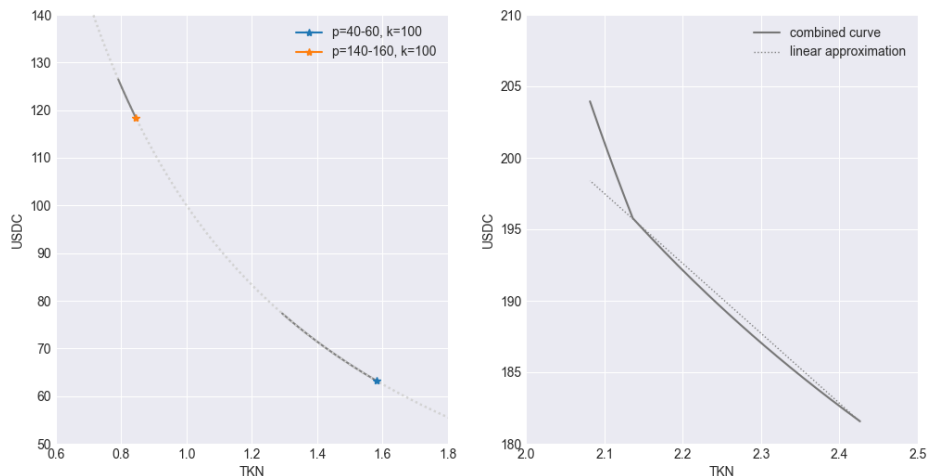


Figure 2.5: *Combining two invariant curves.* The left panel shows two equally sized, levered invariant curves covering disjoint price ranges. The right panel shows the combined invariant curve (the dotted straight line shows curvature of the combined curve).

To finish this section, we show some examples of problematic curves. In principle we could have chosen figure 2.4 for this, but for clarity of exposure we use here a different set of numbers. In figure 2.5 we show two curves that cover non-overlapping price ranges on the same pair. The ranges are relatively wide, and therefore, the prices change substantially within the curve. On the left hand panel we show the invariant function of the constituent curves, and on the right hand one we show the combined invariant curve. We have also drawn a straight line as a benchmark for the right segment of the curve, showing that the actual combined curve is indeed not straight¹². What will happen in this case is that for post-arbitrage market prices between 40-60 and 140-160 the solution is an interior solution on one of the curves (left) or curve segments (right), and for prices below 40, between 60-140 and above 160 the solution is a corner solution where first

¹²Compare the curvature of the solid black line against the straight dotted line in the right curve segment

one and then the other curve flips its liquidity to the other boundary. Depending on the regime we are in, a gradient or simplex method is better suited to find the solution. See the appendix A for a discussion of a closely related geometric problem in higher dimensions, the “radome optimization problem”.

3 Marginal price optimization

We have seen in section 2, that the arbitrage and routing problem is a convex optimization problem, and that we therefore should be able to solve it using standard convex solvers. We have also seen in section 2.3 that there are potential pitfalls with respect to levered curves, where convergence may be problematic. For us, this was particularly problematic, because with the open source solvers of the CVXPY package we used [8], we often were not able to determine why the algorithm failed on a viable scenario, and what, if anything, we could have done to make it converge. Ultimately, we were not able to make them work reliably enough to work in the ArbFastLane [15] product, which motivated the development of an alternative method. This new method is the main focus of this paper: the Marginal Price method for arbitrage finding (and routing). It is similar to solving the conjugate convex problem proposed in [12] which was published around the time we put the finishing touches on our method, and it is based on financial rather than pure mathematical reasoning and somewhat further optimized for performance.

In this section, we describe the method starting from mathematical first principles. For this, we first define the mathematical framework and fix the notations for describing AMMs (section 3.1), and then we do the same with respect to arbitrage transactions (section 3.2). In section 3.3, finally, we move on to our central result – defining the *Marginal Price Formulation* of the arbitrage problem in definition 18, and showing the equivalence with its *Convex Optimization Formulation* from definition 3, in what we refer to as the *Core Equivalence Theorem*, theorem 19.

3.1 Definitions and results related to AMMs

Definition 4 (Token baskets, Overlap, Larger/Smaller). *If we have a market of tokens $i = 1 \dots N$ we define a **token basket** $\mathbf{x} = (x_i)$, $x_i \geq 0$ as a vector of non-negative numbers corresponding to the token holdings in that basket. Two token baskets \mathbf{x} and \mathbf{y} are **non-overlapping** if $\forall i : x_i = 0 \vee y_i = 0$, otherwise they are **overlapping**.*

*A token basket \mathbf{y} is said to be **larger than** a token basket \mathbf{x} (denoted $\mathbf{y} > \mathbf{x}$) iff $\forall i : y_i \geq x_i$, and $\exists i^* : y_{i^*} > x_{i^*}$. The definitions of **smaller than** and **larger/smaller or equal** are analogous.*

It must be understood that the relation $\mathbf{y} > \mathbf{x}$ only introduces a *partial order* on token baskets: for example there is no relation between a basket that holds 1 WETH and one that holds 1,000 USDC.

Definition 5 (Direction). *The **direction** of a token basket \mathbf{x} is the equivalence class of token baskets that only differ from \mathbf{x} by a scalar factor λ . In other words, if $\mathbf{x} = (x_i)$ is a token basket then the direction of \mathbf{x} is the set $\{\lambda \cdot \mathbf{x} = (\lambda x_i) \mid \forall \lambda \neq 0\}$. We call the set where $\lambda > 0$ the **positive direction** and the set where $\lambda < 0$ the **negative direction**.*

Definition 6 (Non-improving prices). *If we have an entity that exchanges a token amount $x > 0$ into an amount $y > 0$ of a different token then we define the **marginal price** at location x in units of y as the derivative $p_{\text{marg}}(x) = \frac{dy}{dx}(x)$. Marginal prices are referred to as **non-improving** if whenever $x_2 > x_1$ then $p_{\text{marg}}(x_2) \leq p_{\text{marg}}(x_1)$.*

*This definition can be extended to token baskets in the obvious manner¹³, and if the non-improving prices condition holds for all token baskets \mathbf{x}, \mathbf{y} then we define this as **non-improving prices in every direction**.*

In other words, non-improving prices mean that the price for the “second dollar sold”

¹³We can reduce the multi-dimensional problem to a one-dimensional one by choosing two non-overlapping directions represented by \mathbf{x}, \mathbf{y} where \mathbf{x} represents the inputs and \mathbf{y} the outputs. If we fix the multiplier λ_x then the AMM will determine the multiplier λ_y such that it considers the exchange of $\lambda_x \cdot \mathbf{x}$ against $\lambda_y \cdot \mathbf{y}$ as fair. Non-improving prices in this context means that the “marginal basket exchange rate” $\frac{d\lambda_y}{d\lambda_x}$ is decreasing in λ_x , ie whatever $\mathbf{x}, \mathbf{y}, \lambda_x$ we have $\frac{d^2 \lambda_y}{d\lambda_x^2} < 0$

cannot be better than the one for the “*first dollar sold*”, both for tokens and token baskets. However, the prices can be the same.

Definition 7 (AMM). *An Automated Market Maker, short **AMM**, operating within a market of tokens $i = 1 \dots N$, is formally defined as an entity that exchanges a token basket \mathbf{x} against a non-overlapping token basket \mathbf{y} at non-improving prices in every direction. An **unlevered** AMM covers the full range of prices $(0, \infty)$ in every direction¹⁴. Any AMM that does not satisfy this condition is referred to as a **levered**.*

AMMs can be **bi-directional** if they trade in both directions and traded tokens automatically move “to the other side of the curve”, or they can be **directed** if tokens can only be traded once. Bi-directional AMMs can impose **trading fees** or not¹⁵.

Definition 8 (Bonding curves and invariant functions). *An AMM is said to be driven by a bonding curve if, ignoring fees and gas, there exists a function f (the so-called “**bonding curve**” or “**invariant function**”) of all token baskets into the real numbers where the AMM is indifferent between all states that have $f(\mathbf{x}) = k = \text{const}$.*

In other words, if the AMM is currently in the state represented by \mathbf{x} , and the basket \mathbf{y} represents a state such that $f(\mathbf{y}) = f(\mathbf{x}) = k$ then it will accept the basket of all tokens for which $y_i - x_i > 0$ in exchange for the basket of all tokens where $y_i - x_i < 0$.

Proposition 9 (Convexity). *An AMM driven by a bonding curve f exhibits non-improving prices in all directions according to definition 6 iff the function $f(\mathbf{x})$ is convex in all directions corresponding to the tokens the AMM covers, and constant in the others.*

Proof. Firstly, the fact that f must be constant (and is therefore just on the border of being convex) in the directions of tokens the AMM does not cover is trivial. The remainder is a well known result (eg referred to in [6]). To sketch a full proof, in the one dimensional case it is easy to see from the definition of the price p which corresponds

¹⁴Covering the full range of prices means that the function $\lambda_y(\lambda_x)$ is defined for all $\lambda_x \in (0, \infty)$ and bijective

¹⁵Note that financially there is no difference between fees and a bid ask spread, and for directed AMMs the notion of fees – the difference between the buying and selling price of the AMM – does not make sense

to the negative of the first derivative $p = -f'$, and the fact that for a convex function we have the second derivative $f'' > 0$. In the higher dimensional case we note that this must hold in every token direction and can therefore be reformulated with the $\lambda_y(\lambda_x)$ functions defined above. ■

Those definitions coincide with the AMM examples provided in section 1.2 where equation 1.1 is an example for a the bonding curve of a multi-asset AMM operating on token balances vectors \mathbf{x}, \mathbf{y} , and both equations 1.3 and 1.5 are examples for bonding curves of single-asset AMMs operating on single token balances x, y . We note that all those bonding curves are convex. For levered AMMs, the values of x, y have to be restricted to the range covered by the AMM.

3.2 Definitions and results related to arbitrage

Definition 10 (Arbitrage-free). *A market consisting of tokens $i = 1 \dots N$ is **arbitrage free** iff there is no sequence of possible trades that starts with a token basket of \mathbf{x} and ends with a token basket of \mathbf{y} where $\mathbf{y} > \mathbf{x}$.*

Note that in the presence of unlimited and cost free **flash loans** (ie loans that can be taken out in unlimited size for all tokens and that have to be repaid at the end of the transaction) the above condition can be simplified to the requirement that it is not possible to start with a balance of $\mathbf{x} = \mathbf{0}$ and end with a balance of $\mathbf{y} > \mathbf{0}$ where the last inequality is to be interpreted in line with definition 4.

Definition 11 (Circularity). *A set of prices $p(i, j)$ ¹⁶ between tokens $i = 1 \dots N$ is said to satisfy the **circularity condition** iff for all closed loops $(i_1, i_2, \dots, i_l, i_1)$ of any length l we have*

$$p(i_1, i_2) \cdot p(i_2, i_3) \cdot \dots \cdot p(i_{l-1}, i_l) \cdot p(i_l, i_1) = 1$$

¹⁶The price convention is that $p(i, j)$ is the price of token i expressed in units of token j

In other words, the circularity condition states that if we exchange infinitesimal amounts¹⁷ of tokens along any closed loop, then we end up with the same token amount we started with.

Proposition 12 (Arbitrage-free unlevered AMMs). *A set of bi-directional unlevered AMMs that charge no fees and that are operating on a token market $i = 1 \dots N$ is **arbitrage free** iff (1) for each token pair (i, j) and for all AMMs that allow trading that pair they do so at the same marginal price $p_{\text{marg}}(i, j)$ and (2) the marginal prices satisfy the circularity condition of definition 11.*

Proof. Before we move on to prove this we point out that this is a well known result in finance, and we refer to [24] as one of many examples. However, as the proof is directly linked to the main topic of this paper we present it here anyway, in a very condensed form. Starting with (1), we note that bi-directional unlevered AMMs that do not charge fees buy and sell at exactly the same price. Therefore, if we have two AMMs that operate on the same token pair at two different prices $p_1 \neq p_2$ then buying low, selling high would be an arbitrage transaction. Note that here the convexity condition is important, ie the first dollar traded must always be at the best price, otherwise we may be able to get additional arbitrages by trading a larger amount. Similarly in (2), we first note that we can move along the loop in either direction, and resulting price in one direction p_+ will be the inverse of the price in the other direction, ie $p^+ = 1/p^-$. Unless the circular product is unity we can always choose a direction in which the circular product in definition 11 is strictly greater than one, and thus we can make an arbitrage profit by trading along the loop in that direction. This concludes the proof in both directions. ■

Proposition 13 (Numeraire). *A set of tokens $i = 1 \dots N$ with marginal prices $p_{\text{marg}}(i, j)$ satisfies the circularity condition iff there exists a sequence of positive numbers (p_i) , $i = 1 \dots N$, typically referred to as "prices", such that for all token pairs $i, j = 1 \dots N$ we have $p_{\text{marg}}(i, j) = p_i/p_j$.*

¹⁷Infinitesimal amounts because curve-based AMMs will continuously adjust prices to the worse so this condition will only ever hold in the limit; we sometimes in a slight abuse of notation refer to infinitesimal transaction amounts as "first dollar traded"

Proof. Proving that circularity follows from the existence of the p_i is straightforward, replacing $p_{\text{marg}}(i, j)$ with p_i/p_j in definition 11 and observing that all terms cancel out. Going the other way, we define $p_i \equiv p_{\text{marg}}(i, 1)$ as the price of token i in terms of the “numeraire token” 1. For every token pair i, j we can look at the loop $(1, i, j, 1)$. Because it is a closed loop, the product of marginal prices is unity, and therefore we have

$$p_{\text{marg}}(i, j) = \frac{p_{\text{marg}}(i, 1)}{p_{\text{marg}}(j, 1)} \equiv p_i/p_j \quad (3.1)$$

which concludes the proof. ■

We note that the numeraire p_i is only unique up to a multiplicative constant λ , meaning that if p_i is a numeraire then $\bar{p}_i = \lambda p_i$ is also a numeraire that yields the same prices. If for a given token i^* we chose the constant λ such that $p_{i^*} = 1$ then we refer to this as “token i^* being the numeraire”. Given the above proposition we define the concept below that allows us to abstract prices from a specific numeraire:

Definition 14 (Price vector). *Given a set of tokens $i = 1 \dots N$ we define the **price vector** $\pi = (\pi_1, \dots, \pi_N)$ as the vector of prices in a specific numeraire. We also define the associated **price function***

$$\pi_{ij} = \pi_i/\pi_j$$

We define an equivalence relation between price vectors that we denote “=” where two price vectors π^a and π^b are equivalent iff their price functions coincide, ie

$$\pi^a = \pi^b : \iff \forall i, j : \pi_{ij}^a = \pi_{ij}^b$$

meaning the ratios $\pi_i^a/\pi_j^a = \pi_i^b/\pi_j^b$ are the same .

The purpose of the above definition is to abstract the price information in a fully arbitrated market. We note that the price vector π itself should never be used directly

because it is only defined up to a multiplicative constant. Instead, all usage of π should respect the associated equivalence relation which can be assured by always using the associated price function π_{ij} instead of the components p_i .

However, the price vector π is a valid mathematical object that resides in the reduced dimensional space where all prices are positive and where the numeraire token is fixed at unity (ie $\pi \in R_{>0}^{N-1} \times \{1\}$).

At this stage, we are ready to move on to prove a more general proposition that covers levered and unlevered AMMs:

Theorem 15 (Arbitrage-free AMMs). *A set of levered or unlevered AMMs $\nu = 1 \dots M$ operating on a token set $i = 1 \dots N$ is **arbitrage free** iff there exists a vector of prices p_i so that for every AMM trading a token pair i, j the marginal price satisfies $p_{\text{marg}}^\nu(i, j) \overset{\rightarrow}{\equiv} p_i/p_j$ where the symbol $\overset{\rightarrow}{\equiv}$ indicates that the marginal price on the left is the closest approximation to p_i/p_j within the set of attainable prices of AMM ν .*

Proof. First we note that, in case of unlevered AMMs, this proposition reduces to proposition 12 because (a) the closest attainable price will simply be p_i/p_j , so (b) all AMMs exchanging tokens i, j will be set at the same price p_i/p_j that (c) satisfies the circularity condition in definition 11 because of proposition 13. For a levered AMM, we firstly note that if the current marginal price is not at a boundary, for small trades the levered AMM behaves like an unlevered AMM, therefore the same reasoning applies and its marginal price must be at p_i/p_j as in the unlevered case. If the price of the AMM was at the boundary away from p_i/p_j then someone trading against the AMM could buy low at p_i/p_j from another curve and sell high into the AMM stuck at the far boundary, thereby moving the price closer towards p_i/p_j . The only point where this trade is not possible is at the boundary closest to p_i/p_j because at this point the AMM will no longer buy. ■

We next we define the *price response function* (“**PRF**”) that indicates how an AMM – or a set of AMMs – responds to a change in price(s):

Definition 16 (Price response function). *Given a set of AMMs $\nu = 1 \dots M$, a set of tokens $i = 1 \dots N$, the **individual PRF** ρ_ν of AMM ν is an equivalence-respecting¹⁸ function that maps a price vector π to a set of token changes*

$$\rho_\nu(\pi) = (\Delta x_{\nu 1}, \dots, \Delta x_{\nu N})$$

The **aggregate PRF** of a set of AMMs ρ is the sum of the individual PRFs

$$\rho(\pi) = \sum_{\nu=1}^M \rho_\nu(\pi)$$

By convention, outflows from the AMM are negative, and inflows are positive, therefore the pre-trade balances \mathbf{x}^{pre} and post trade balances \mathbf{x}^{post} satisfy

$$x_{\nu i}^{\text{post}} = x_{\nu i}^{\text{pre}} + \Delta x_{\nu i}$$

Arguably, the PRFs are the most important financial objects that we are dealing with. They are equivalent to, but more financially relevant than, the usual invariant functions in equations 1.1, 1.3, and 1.5. For a traditional AMM without fees they are path independent, meaning that aggregating the PRF results over any price path $\pi^1, \pi^2, \dots, \pi^N$ is the same as going directly to π^N , the end point¹⁹. However, in the presence of fees, things change. Firstly, longer paths lead to a higher fee bleed. Moreover, if fees accumulate on the curve, the invariant curve changes and therefore, so does the PRF. Finally, in a directed AMM like Carbon DeFi, curves do not automatically *reload*²⁰, so in this case the PRF is usually highly path-dependent.

Definition 17 (Trade instructions). *A **trade instruction matrix** ("**TIM**" or simply "**trade instructions**") for a set of AMMs $\nu = 1 \dots M$ operating in the token set $i =$*

¹⁸In line with definition 14

¹⁹This follows directly from the derivation of the PRF from an invariant curve

²⁰Except via the associated counter curve in the Carbon DeFi "Strategy", if so desired

$1 \dots N$ is a matrix $(\Delta x_{\nu i})$ that describes the flows of token i into (positive) and out of (negative) the AMM ν . A TIM is called "respecting a set of self financing constraints" if its aggregate over all ν fulfils the constraints from equation 2.9. It is called an "**arbitrage TIM**" if it fulfils the arbitrage SFC in equation 2.8. In those two cases we refer to $\sum_{\nu} \Delta x_{\nu i}$ as the **result**²¹ of the arbitrage finding or routing process. In case of a pure arbitrage, the negative result (a positive number) is also referred to as the **arbitrage profit**.

3.3 The Core Equivalence Theorem

We are now ready to present the mathematical core of this paper, the claim that the marginal price optimization problem described in this paper which forms the basis of operations for the FastLane Arbitrage bot [15] is equivalent to the convex optimization problem described in section 2 based on [6]. To do this, we first formally define the "Marginal Price Formulation" of the problem:

Definition 18 (Marginal Price Formulation). *The "**Marginal Price Formulation of the Arbitrage Problem**" is the root finding problem to identify the price vector π that satisfies the **arbitrage condition***

$$\rho(\pi) = -\lambda e_0$$

where e_0 is the unit vector of the zeroth vector component²² and the "result" (in the sense of definition 17) $\lambda \geq 0$ is a scalar determined by the algorithm via the trade instruction matrix that we will show to be non-negative below in proposition 20.

Note that whilst the optimal routing problem is out of scope in this paper we still want to record the fact that for routing the above equation will become

²¹This terminology is driven by the usage of the term "result" within an convex optimization context

²²Again like in the footnote to equation 2.10 the choice of token 0 is WLOG and for simplicity of presentation only; this condition states that this is a pure arbitrage transaction where the profits, if any, are taken in token 0

$$\rho(\pi) = -\lambda e_0 + \mathbf{x}$$

where the vector \mathbf{x} are the desired in and outputs in tokens other than 0 like in equation 2.9.

We now show that the above *Marginal Price Formulation* is equivalent to the *Convex Optimization Formulation* that was the subject of section 2, and specifically defined in definition 3. En passant we note that this is essentially the well-known result from convex optimization theory linking a problem and its conjugate as used in [12], but as our focus is on finance as opposed to pure mathematics we want to provide a self-contained proof more financial proof.

Theorem 19 (Core Equivalence). *The problem of finding arbitrages (or route optimally) in a set of AMMs in the Marginal Price Formulation as described in definition 18 is equivalent to the Convex Optimization Formulation as described in definition 3. Specifically, the trade instruction matrix (and therefore the arbitrage profit) obtained by both formulations will be the same.*

Proof. To prove the above, we start with creating a list of items where the two formulations coincide, and where they differ. The formulations coincide in the following items

1. They are solving the same arbitrage finding problem as presented in definition 1²³.
2. They start with a set of AMM curves satisfying invariant equations along the lines of definition 8, and holding the associated amounts of tokens pre-arbitrage.
3. They seek a set of post-arbitrage token holdings, or equivalently a trade instruction matrix along the lines of definition 17, that implements the arbitrage transaction, and that satisfies the self financing constraints according to equation 2.8.

²³For ease of presentation we here focus on arbitrage alone and leave the simple extension of the proof to routing application to the reader

The convex optimization formulation (“COF”) and marginal price formulation (“MPF”) differ in the following way:

1. The COF seeks to minimize a target function in line with equation 2.10 whilst the MPF seeks to find the root according to definition 18.
2. The COF algorithm operates directly on the AMM token holdings x_{ν_i} whilst the MPF algorithm operates on a marginal price vector π_i according to definition 14.

To prove equivalence, we have to either (a) show that they are the same, or that (b) the MPF solution satisfies the COF conditions and vice versa. We start with a non-rigorous argument for (a) by pointing out that both are solving the financial real-world arbitrage problem 1 that, in a non-path-dependent environment, has a unique solution²⁴. However, we have pointed out before that Carbon DeFi positions introduce path dependence, and we can only accept this as a proof when no directional curves are in the curve set.

For proving the theorem along the lines of (b) we first show that the optimal solution in the COF framework satisfies the MPF conditions. For this we point out that if marginal prices were not to satisfy the price conditions in proposition 12 then additional profits could be generated by “buying low selling high” and therefore the convex optimization process had not worked as advertised²⁵.

Now we go the other way and show that a solution of the MPF satisfies the constraints of the COF and minimizes the target function. By design, the MPF solution satisfies the positivity constraints from equation 2.1, the self-financing constraints from equation 2.8 and curve constraints from either equation 2.2 or 2.3. To show that this also minimizes the (negative) target function we note that by construction the state of the market is arbitrage free, and the existence of a state with a bigger outflow under the same self-

²⁴Unique in the sense that if there were multiple solutions one could always trade from one to the other so any algorithm that gets stuck on a sub-optimal solution does not in fact solve the arbitrage problem; there can, however, be cases where more than one set of trade instructions yields the same arbitrage profit in which case both algorithms may find either of them depending on starting conditions and algorithm details

²⁵We had some concern in cases where *profit repatriation* was an issue, but as we have shown in detail in appendix B that is is not in fact the case

financing constraints would imply that there were arbitrages available in the initial state.

■

Proposition 20 (Existence and uniqueness). *A solution to the routing problem based on equation 2.9 may or may not exist, depending on the state of the AMMs and the routing constraints \mathbf{x} . A solution to the arbitrage problem based on equation 2.8 (ie, $\mathbf{x} = \mathbf{0}$) always exists and the result parameter λ from definition 18 will be positive, or zero if there is no arbitrage opportunity. If a solution exists, it will be unique.*

Proof. For the *may or may not exist* part, nothing needs to be proved. All other properties follow directly from the Core Equivalence Theorem 19, and the fact that the empty solution (zero everywhere) will either dominate the convex solution, or be the solution. ■

We want to briefly elaborate on the *may or may not exist* part, using financial arguments. Firstly, unlevered curves can take up any number of tokens, so any routing constraint pushing tokens into the system will not usually be a problem. Provided there is a route from all inputs to the desired output token, the routing problem will always have a solution. Constraints taking tokens out of the system are limited by the number of tokens available in the system however, so if this number is being increased, at one point there will no longer be a solution. Tokens that only live on levered curves will also have a maximum amount that can be pushed in.

4 Implementation and convergence

Whilst the marginal price algorithm is in principle the same on token pairs and on token sets containing more than two tokens, there are important numerical differences. Most importantly, on token pairs the problem is a one-dimensional root finding problem, and according to the intermediate value theorem [1] we are guaranteed to find a root²⁶ if we can bracket it. Convergence will be in logarithmic time – every step will increase the

²⁶Or rather, a root location, if we also consider step functions that may not technically have a root, a case that is of practical importance for us; see appendix D.1 for details

precision by a factor of two.

As we discuss in appendix D.1.4, in higher dimensions there is no equivalent to the intermediate value theorem, and therefore no equivalent to the bisection method that is guaranteed to converge. In fact, a priori it is not clear that a solution even exists: we have a function $f : R^n \rightarrow R^n$ and we are looking for a point \mathbf{x} such that $f(\mathbf{x}) = \mathbf{0}$. In general, such a point does not always exist, and if it exists it is not clear that it is unique.

Having said this – our problem is more benign than the general mathematical framework may suggest. After all, we are solving a real world problem in finance, and as shown in [6], the problem is convex and therefore has a unique solution. Specifically, the arbitrage problem is always dominated by the *null solution*, so either either a proper arbitrage solution exists, or *do nothing* is the formal solution to the arbitrage problem. The issue is therefore less the question of existence and uniqueness²⁷, but rather the question of how to find the solution within a reasonable amount of time.

We have split the discussion into multiple parts. First, we discuss the implementation in the case of a single token pair using bisection in section 4.1. We then discuss the generic case using Newton-Raphson / gradient in section 4.2, and finally we deal with the topic of convergence in section 4.3.

4.1 Marginal price optimization on token pairs

On token pairs, the arbitrage problem boils down to finding a single price where the net flow of all other tokens than the target token is zero for arbitrage, or a specific number for optimal routing²⁸.

This means that in two dimensions, our general root finding problem without fees looks

²⁷Again, financially it is clear that trade instructions cannot be unique in the general case; for example, consider two zero-slippage curves covering the same pair where any routing of the required amount through the two curves will be a solution

²⁸The marginal price routing algorithm is the one used when trading on Carbon DeFi via the canonical user interface

generally like the different graphs depicted in figure 4.1: an unlevered curve is a simple convex line (blue, 1), a single levered curve is a convex segment in between two flat areas (orange, 2), and multiple levered curves at different prices correspond to a series of convex segments separated by flat areas (green, 3).

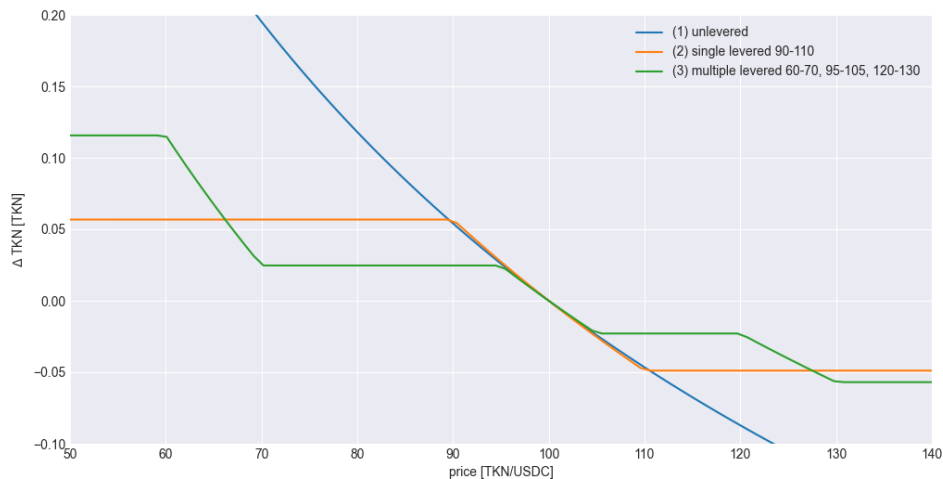


Figure 4.1: *Price response function with no fees.* Price response function, defined as change in token amounts against price for (1) a single unlevered curve, (2) a single levered curve, and (3) multiple levered curves, all curves with no fees and all at current price $p = 100$.

Note that if we include fees the picture changes considerably in that we get a flat area inserted at the current price point which depicts the boundary between buying and selling. The width of the flat area is the current price multiplied with the percentage fee charged. This is shown in figure 4.2 for an unlevered curve in the left hand panel and a levered curve in the right hand panel.

For one dimensional root finding problems, there are fundamentally two methods

- the bisection or bracketing method described in appendix D.1, and
- the Newton-Raphson or gradient descent method described in appendix D.2.

As discussed in appendix D.1.3, the bisection method is extremely robust in that it will

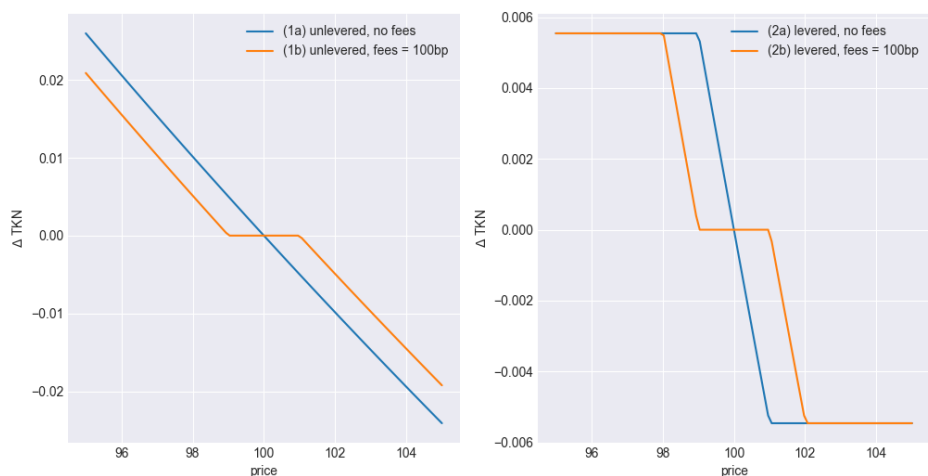


Figure 4.2: *Comparison of price response function with and without fees.* Price response function, defined as change in token amounts against price for (1) unlevered curves, (2) levered curves, (a) without and (b) with fees, all at current price $p = 100$.

either fail right from the start (because the bracketing did not yield two points with an opposite sign), or it is guaranteed to converge to the location of either a root in case the function is continuous (cf left hand panel in figure D.1), or a *root location* where the target function changes its sign in case the function is not continuous and jumps across the x-axis (cf right hand panel in figure D.1).

Depending on the shape of the function, the Newton-Raphson method can be much faster than the bisection method. As we discuss in appendix D.2.1, if the function is linear, convergence is in one step. Generally, on convex functions convergence is fast regardless of the starting point (see figures D.4 and D.5 for a few examples). However, for functions that change convexity, or that are not continuously differentiable, a number of bad things can happen, notably the algorithm can go into an infinite cycle (see figure D.5 bottom right panel), or the new sampling point can be catapulted to “infinity” when the function is very flat at the current sampling point, and depending on the shape of the function it can be impossible to recover from that.

For example, consider the green function (3) in figure 4.1 in the price area around $p \simeq 80$.

The function is flat and therefore any gradient descent will fail. We could regularize the function somewhat (eg by adding a small slope to ensure that the gradient is never zero). However, even this regularization would lead the algorithm very far out, into another flat area, from where the regularization would lead it back. In this case we can have either of two eventual outcomes: the algorithm may eventually end up in the price area of the curve that contains the root²⁹, or it may end up in an infinite cycle. In practice, we will most likely see a large number of iterations and we will run into our *maximum iteration* boundary. In any case – those kind of scenarios are extremely inefficient for a Newton Raphson algorithm: either it takes a long time to converge, or it takes even longer until we decide that it does not converge in the allotted time.

Generally in the pair case, the improved speed of the Newton-Raphson method in our experience does not outweigh the risk of non-convergence, so we exclusively use a bisection method when we deal with arbitrage or routing within a single token pair.

We do need to qualify the robustness claim made above though because, for non-continuous functions, it only applies in *price-space*. However we seek to specify transactions that live in *token-amount-space*, so convergence in price-space is not enough. This is not an issue with the bisection algorithm specifically, but rather with converting a token space problem into a price space problem as is the foundation of the marginal price method. It is particularly annoying, however, in case of the bisection method, because it somewhat torpedoes the robustness properties of this algorithm.

The functions that pose problems are those that are discontinuous at their root location (ie that jump from positive to negative or vice versa). In practical applications this also includes functions that are *numerically discontinuous*, with which we mean functions that have such a steep gradient that, within the resolution of the algorithm, they appear to be discontinuous. Those functions are easily identified: they are what in Carbon DeFi [31] we refer to as “*limit orders*” (ie orders where the parameter $A = 0$ and where the

²⁹This is the equivalent of ending up by chance on the correct face of the radome in the example of appendix A

start and end price are the same). In practice, very narrow ranges with $A \gtrsim 0$ also pose a problem, because they are what we referred to as “numerically discontinuous” above³⁰.

In the introductory section 1.3 on optimization, we have introduced, in equation 1.7, the *convolution method* to regularize a function. We could apply this method here, but in practice we find it easier to enforce a minimum width for limit orders. Specifically, we enforce values of A, B so that they satisfy the condition above with $\varepsilon_0 \simeq 10^{-6}$, and we adjust both A and B if this is not the case, ensuring that the adjustment is such that the effective price of the order, when fully executed, remains the same.

4.2 General marginal price optimization

We now move on to the higher dimensional case, ie everything where more than two tokens are involved. As discussed in appendix D.1.4, there is no equivalent of the bisection method in dimensions higher than one, so we are forced to use a multi-dimensional Newton-Raphson method as described in appendix D.2.3. If we have $N + 1$ tokens $i = 0 \dots N$, this algorithm works as follows:

1. Compute the $N \times N$ Jacobian matrix J_{ij} , consisting of the derivatives of all N function values – the self-financing constraints of all but the target token according to equation 2.8 or 2.9 – to all N prices in the price vector defined in definition 14, according to equation D.6.
2. Invert the Jacobian to solve the linear approximation of the function, as described in equations D.7 and D.8.
3. Update the price vector according to equation D.9, taking into account the learning rate η if need be.
4. Repeat until convergence or failure (maximum iterations or away from reasonable domain).

³⁰Note that technically A has the units of the square root of a price, so it is not a scale free number, and the correct condition for a range being “small” is along the lines of $A/B < \sqrt{\varepsilon_0}$ where ε_0 is some small number

This algorithm looks deceptively easy, but for it to work in a production setting, a number of points need to be considered, most importantly the following:

Log Prices. We initially implemented the algorithm using actual prices. This ran into a number of issues, most importantly that sometimes the algorithm ended up in a situation where the price was negative. Also, because price levels in crypto can range from below 10^{-6} to the dollar to almost 100,000, the numerical conditioning is not ideal, in particular for calculating the derivatives of the price response function (definition 16) for the Jacobian. We therefore switched to log prices; we define $\mathbf{x} = \log \pi$ and we perform all calculations for the algorithm in the log space \mathbf{x} , not in the price space π .

Calculating Derivatives. We calculate the Jacobian using perturbations. Because we operate in log space, those are effectively percentage-perturbations, which means we don't need to worry much about the size of the calculation stencil. Although, we need to be somewhat careful if we are at the price boundary of a levered position to ensure that (a) the algorithm does return a result there, and (b) the result is sensible³¹.

Curves with no closed form solutions. Because we calculate the derivative of the price response function (definition 16) numerically via perturbation, and this calculation is at the core of the algorithm, it is important that this calculation is fast and consistent³². Calculating derivatives from something that itself relies on numerical approximations is often slow and error prone – so in cases where we do not have a closed form solution for the PRF of a specific AMM, we approximate the curve with sufficient number of levered constant product AMMs placed next to each other and use those for the calculations.

Singular Jacobian. The Jacobian can become singular, in which case the naïve algorithm fails. We have implemented a fallback algorithm that inverts the Jacobian only on its image, and does not attempt inversion on its null space. This improves perfor-

³¹We currently calculate derivatives along the blue (sum first) path we will define in diagram 5.1 in the next section, section 5. Please refer to the discussion in that section for the implications thereof

³²Please refer to the next section, specifically 5.4, for a discussion how the calculation of the Jacobian is the main numerical effort of the current algorithm

mance in higher dimensional cases, because there is at least a chance that the algorithm either ends up in a non-singular place, or that the singularity corresponds to prices that ultimately do not matter for the arbitrage problem at hand. Note that singularities typically occur if at a certain price level there are no curves that allow trading the pair corresponding to that price. Because of the market structure on crypto markets, where most AMM curves are against one of (W)ETH, WBTC or a USD stable coin, this is particularly pertinent if an unusual target token is chosen, which in turn suggests that it may be better to choose one of the aforementioned tokens as target token.

Learning rate. We have experimented with changing the learning rate η to improve convergence, but we found that it did not make a significant difference. In reality, the biggest issue is that, because of lack of liquidity in a certain price region, prices are catapulted towards infinity, and catapulting them to towards “ η times infinity” does not seem to lead a significant improvement. On the other hand, choosing $\eta < 1$ is costly. In figure D.6 in the appendix we have illustrated the impact of the learning rate η on the Newton Raphson algorithm. Abstracting the findings from this further we have plotted in figure 4.3 the *slowdown factor* n for a given *convergence level* d as a function of the learning rate η . The convergence level $d \in (0, 1)$ describes the residual distance to the real solution as a function of the original distance (eg $d = 0.01$ means that the distance has been reduced by a factor of 100). The slowdown factor n is the number of iterations required to reach this level of convergence. We note that that slowdown factor is a real cost: running the algorithm is computationally expensive, and the slowdown factor n goes directly to the running cost bottom line, and it can also affect latency which matters on fast chains.

Convergence criteria. We have initially used a *relative* convergence criteria (ie that the algorithm does not change prices any longer). In some ways this is a good criterion, because we operate in log space, so the criterion is effectively the *average percentage change*. The issue is that the algorithm in this case relatively often indicated it had converged, even though it had simply ended up in a region with no liquidity at all and,

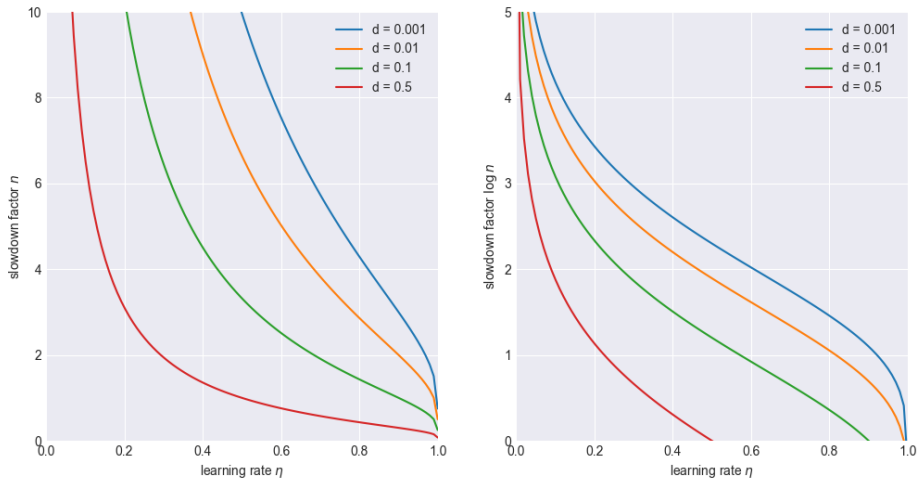


Figure 4.3: *Slowdown in convergence as a function of the learning rate.* Slowdown factor (ie number of iterations required) n to achieve various convergence levels d as a function of the learning rate η , regular (left) and log scale (right).

therefore, where the Jacobian was flat zero. We could have tested for this, but we ultimately chose an *absolute* criterion along the lines of “*average violation of the self-financing constraints < 1 USD*”, which is more financially meaningful. The downside in this case was that we always needed to provide USD prices to the algorithm, even if no USD curves were involved in the arbitrage problem at hand. Also, divergence can take longer if the algorithm is stuck close to infinity – relative convergence would break right away, falsely claiming convergence. Absolute convergence will eventually rightly report non-convergence, but it will take longer to do so because it will run empty cycles.

Convergence issues. Regardless of the criteria used, the algorithm sometimes diverges, even though a solution exists. We have already discussed the issue in relation to the convex optimization algorithm in section 2.3, and whilst the marginal price algorithm converges better, it still has a substantial failure rate when very thin curves are involved.

Decomposition and linearization. We will discuss the linearization and routing problem in our upcoming paper on transaction decomposition linearization [27], so here we present just a brief introduction to the topic. As we already pointed out in the ex-

ample discussed in the intro to section 4, the algorithm generally creates a set of trade instruction that touches many, and possibly all, curves. Having a transaction with so many curves has two drawbacks. Most importantly, the more curves are involved, the more likely the whole transaction is to fail because the blockchain state has changed by the time the transaction is included. Additionally, if there are limited flashloan opportunities and we have only limited token amounts, linearization³³ of the transaction can be complex. The latter problem can be dealt with, but the former remains: we usually want to decompose the transaction into smaller ones, and prioritize their submission based on profitability and complexity.

4.3 Convergence

Convergence of the marginal price algorithm is significantly better than that of the convex optimization algorithm from [6]. For example, the example discussed in section 2.3 converges well to the same result as in table 2.4 without need for a sentinel curve like in figure 2.4. However, even the marginal price algorithm can run into convergence issues. We have thus far identified two scenarios that do lead to divergence:

- **escape scenario:** the gradient catapults the algorithm into a region where no curves are located, at which point it is either blocked, or jumps around erratically
- **loop scenario:** the algorithm enters an infinite loop without ever converging to a solution, or at least not within the maximum iterations allowed

Both scenarios are shown in figure 4.4. All panels depict price response functions of different scenarios, and in all case the solution $dx(p) = 0$ is found in segment (2) and convergence is fast provided the algorithm starts in, or ever reaches, segment (2). In each of the cases however, whenever the algorithm starts in region (1) it will diverge.

The left and middle panels show escape scenarios. In the left panel, the curve segment (1) is relatively steep so the next point will be in segment (3), close to segment (2).

³³The term “linearization” refers to the process of creating a transaction (based on own token holdings or flashloans) that can be executed in a linear manner without any intermediate token balances ever falling below zero

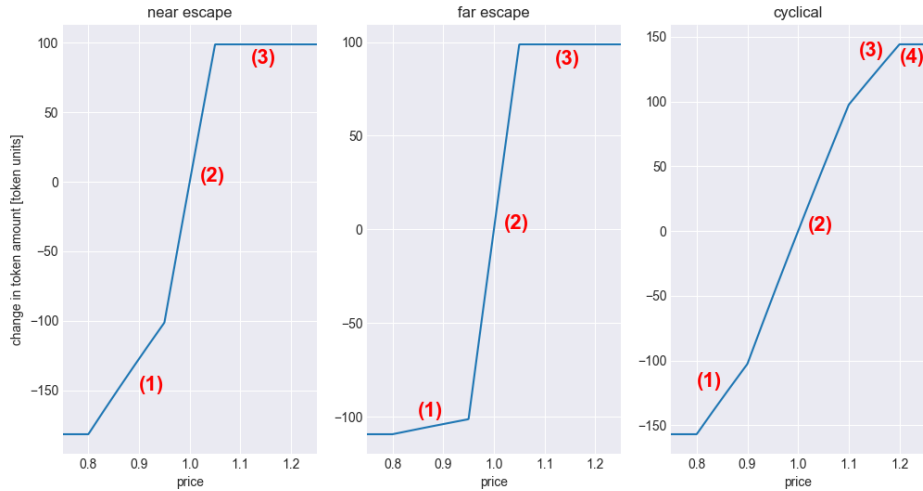


Figure 4.4: *Divergent scenarios for the marginal price optimizer.* The panels above show price response functions where the result is in segment (2) and they diverge when starting in segment (1). The two left panels escape to segment (3), the left one closely, the middle one far away. The right panel enters into an infinite loop (1), (3), (1), etc.

In the middle panel, the curve is very flat and the escape is towards infinity. In those particular cases this does not make a big difference – both algorithms will detect a zero gradient, at which point they will fail. What this shows however is that a learning rate η (as discussed in section 4.2) may or may not be helpful: Whilst in the left panel, an $\eta \simeq 0.8$ would bring us into segment (2) from where we would converge, in the middle panel we would need a really small η to not end up in the empty region (3). However, this would be too detrimental for the overall speed of convergence of the algorithm, as discussed in appendix D.2.2.

The right panel shows a loop scenario similar to the one shown in the bottom right panel of figure D.5. Here, we have three curve segments, so (4) instead of (3) indicates the segment without curves. Here, if we start in segment (1), the algorithm will bring us to (3). From there, we will return to (1) and the cycle restarts. Depending on the exact starting point and shape of the curve, the algorithm may eventually escape to segment (4) or its counterpart on the left, may hit segment (2) and will converge, or it may

be stuck in an infinite loop. In reality this does not usually matter because we cannot afford to run the algorithm until we find out, so each of those three cases will hit the maximum-iterations boundary.

Whilst neither of the scenarios converges, in the above two dimensional case there is an important difference: the escape scenario diverges very quickly – as soon as the algorithm enters the empty space it will detect a zero gradient, at which point it will know it has failed and will terminate. The loop scenario is harder to detect, and in fact we only detect it via hitting the maximum iterations threshold. This of course is expensive, and careful management of this boundary is important because it will significantly impact the performance of the algorithm. We note that the bona fide escape scenario is relatively rare: whenever there is an unlevered curve present in the analysis, the gradient will never be fully zero, in which case we will end up in a variation of the loop scenario.

In higher dimensions the issues are different, except that one can have a convergent and all types of divergent scenarios present at the same time, depending on the direction. We currently only terminate if the Jacobian is zero. If it is singular – meaning that we are in the empty space in at least one of the directions – we instead invert the Jacobian on the invertible sub space only, on the hope that this returns us to a region where the entire Jacobian is invertible again. We are not currently certain whether or not this is the right choice because if we do not quickly return to the core region of convergence we simply waste more iterations on the problem before we diverge anyway. Currently we are leaving it in because we value convergence over speed.

5 Performance comparison

In this section, we report the results of our performance comparison between the different algorithms. The software and hardware details are in table 5.1. The performance of this machine is comparable to the cloud servers we use in the production environment, so the numbers, which range from milliseconds to seconds, are indicative of what we can expect there.

	version
system	
MacBook	Air M3 2024
MacOS	15.0
RAM	16 GB
python	3.12.4
cvxpy	1.5.2
numpy	1.26.4
pandas	1.5.3
matplotlib	3.9.1
networkx	3.3

Table 5.1: System configuraton for analysis

Times are measured using simple wall clock time from start to end of the calculation, including the profiling of the code in 5.4 which used instruments introduced into the code that recorded wall clock readings along important way points of the execution and then aggregated the results into an overall *time-spent-per-stage* reading. We are well aware of the theoretical limitations of this approach, and we have taken measures to address those. For example, for measuring short running processes we have repeated the measurements up to 10-100x. The ultimate size of the effect observed in the results suggests that those measures were sufficient for our purposes: our core result shows a 20x to 100x+ improvement for the marginal price algorithm over the convex ones from [6]³⁴, which is beyond any noise or bias that could possibly be introduced by our measurement protocol.

The contestants in our line up are the following algorithms:

1. Marginal Price optimization using a bisection algorithm as described in appendix D.1, which we call the **pair mode** in our implementation because it only works if all curves are operating on the same pair of tokens
2. Marginal Price optimization using Newton-Raphson / gradient descent as de-

³⁴As it was published around the same time as we put the finishing touches on our algorithm we have never implemented the conjugate algorithm described in [12] so we cannot directly compare the two, but the performance improvement we achieve against [6] that we are significantly faster, albeit not by the same margin

scribed in appendix D.2, which is what we call the **full mode** because there is no restriction on the number of tokens

3. Convex optimization with CVXPY [9, 13, 8] using the new default solver **Clarabel**
4. Ditto using the older solvers **ECOS** and **SCS** which ex post we group together because their performance here is very similar

5.1 Performance on token pairs

We start the analysis on token pairs, the only arena where all contestants, including our marginal price pair mode, can compete. For this, we run the algorithms on two tokens, and we vary the number of curves from 2 to 2,000. We note that whilst using traditional AMMs even the most crowded pairs will not usually present more than a dozen of curves, we have developed the marginal price algorithm for the use together with the CarbonDeFi protocol [31, 32, 18], where every single trading position is a curve. For busy markets, a few thousand positions is not a particularly high number.

The key results we have obtained for token pairs are summarized in figure 5.1. Note that we limited our charts to 200 curves in this case – our analysis ran further (up to 2,000) but nothing meaningfully different happened there, so we chose the tighter range for a more effective presentation. The left panel of figure 5.1 shows the performance of all algorithms on a linear scale, and the right panel zooms into the two marginal price algorithms only. We make the following observations, most of which are representative for more general cases which we will discuss in the following sections.

Observation 21 (Performance comparison). *When comparing the performance of the different algorithms for token pairs in 5.1, we find a number of key differences:*

1. *The marginal price modes outperform the convex modes by a massive margin, to the point that the curve of the full marginal price mode appears flat in the chart.*
2. *The pair mode is substantially slower than the full mode. The ratio is somewhat volatile but as the right panel shows, the speedup of the full mode versus the pair*

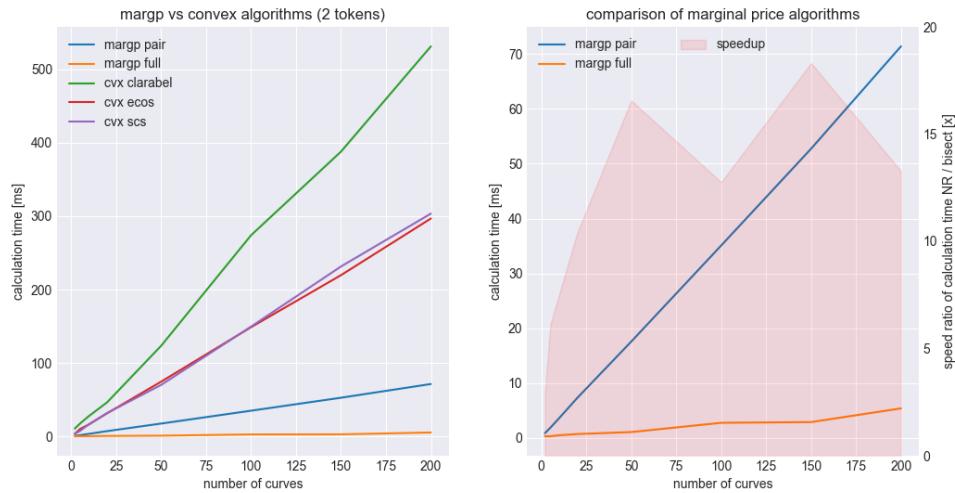


Figure 5.1: *Calculation time versus number of curves (token pairs)*. The left hand panel shows the calculation time in ms for the different algorithms (orange and blue marginal price; the others convex) on token pairs. The the right hand panel shows the same data for the marginal price algorithms only, plus the speedup ratio between the two (red surface).

mode is at least 5-10x, except for the very smallest number of curves where the fixed costs dominate the algorithm.

3. *The convex algorithms group into ECOS and SCS on one hand, and Clarabel, the new algorithm on the other one. None of the algorithms are competitive to even the pair mode, let alone the full mode. Clarabel is performing significantly worse than the older ECOS/SCS.*
4. *None of the convex algorithms display a performance that would be useable for real life arbitrage purposes across a large number of curves – the calculation time required scales approximately linearly in the number of curves, at about 1.5 seconds per 1,000 curves for ECOS/SCS and almost 3 seconds for Clarabel. For comparison, pair mode is at 0.4 seconds, and full mode at about 0.04 seconds per 1,000 curves.*

5.2 Scaling the number of curves

We now look more closely at what happens when we increase the number of curves whilst holding the number of tokens constant. We have run the analysis for different numbers of tokens between 2 and 20. The results we show here are for 10 tokens, and they are representative for what he have seen in the other cases.

The results are presented in figure 5.2 where the left panel is the same chart as in the left panel of figure 5.1 except that the x-axis now goes up to 2,000 curves. Also, as the number of tokens is above two, there is no marginal price *pair mode*. Fundamentally, the results are the same as in observation 21, except that Clarabel seems to perform even worse: whilst ECOS/SCS deteriorate linearly, the curve for Clarabel looks quadratic. At more than 40 seconds to run a single analysis on 2,000 curves it is beyond any usefulness for us in practical settings. It also dominates the chart in the left hand panel to the extent that the performance figures for the other algorithms are hard to read.

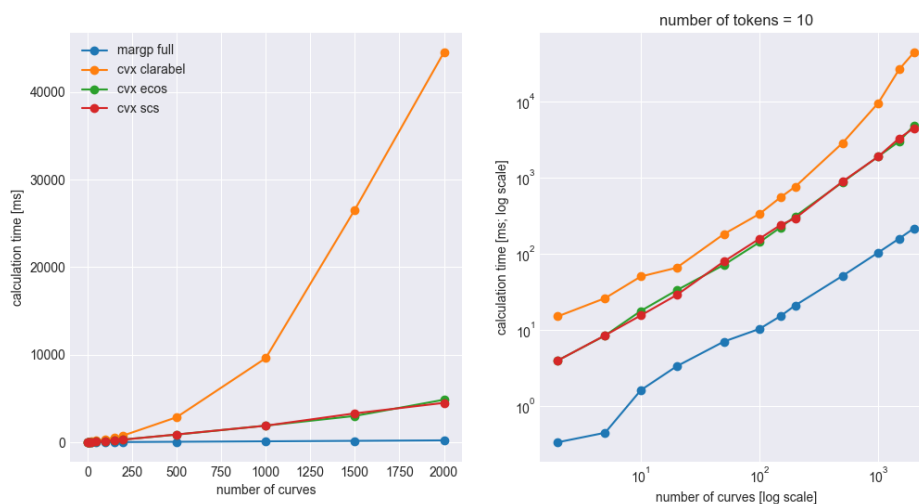


Figure 5.2: *Calculation time versus number of curves (10 tokens)*. Both panels show the calculation time for the different algorithms in a market with 10 tokens as a function of the number of curves. Blue is marginal price full mode, orange is Clarabel, and green/red are ECOS/SCS. The left hand panel is on a linear scale, the right hand panel is on a log/log scale.

We therefore redraw the same chart in the right hand panel of figure figure 5.2 on a log/log scale. The marginal price algorithm is the clear winner, with a consistent performance of about 10ms per 1,000 curves. The ECOS/SCS group is consistently behind by what looks like an order of magnitude along the entire curve, and Clarabel is another half order of magnitude behind that at the start, deteriorating to a full order of magnitude at the large-number-of-curves end of the spectrum.

speedup versus: n curves	clarabel	ecos	scs
10	31.3x	11.0x	9.6x
100	32.6x	13.8x	15.4x
500	56.0x	17.1x	17.4x
1000	92.7x	18.3x	18.3x
2000	206.6x	22.5x	20.9x

Table 5.2: Speedup marginal price versus convex (10 tokens)

We we present the associated speedup numbers of the marginal price algorithm over the convex algorithms in table table 5.2. We see that ECOS/SCS are behind the marginal algorithms by a factor of 10-20x, with the distance getting larger at larger-number-of-curves end. The speedup compared to Clarabel starts at 30x for 10 curves and reaches 200x+ for 2,000 curves, and is most likely getting even worse beyond that. This is making CVXPY’s new default solver definitely not a good choice for this task, even when compared to ECOS/SCS.

5.3 Mathematical interlude

The results of the following section 5.4 have surprised us at first. Before we continue, we need to provide some additional context. As we discuss in a forthcoming paper [27], we only ever use the optimization algorithm for two or three tokens at a time, and we loop over the reasonable token combinations. Therefore, performance of our implementation of the algorithm is not relevant for us for large token numbers, but we do care about the performance for large numbers of curves. This means that in practice we operate in the region covered by section 5.2.

However, when running numbers for this paper, we found that our implementation degrades significantly when the number of tokens gets large, to the point that as shown in figure 5.3 we can go beyond ECOS/SCS. When we looked into this, we concluded that this was an artefact of the way we implemented the algorithm rather than a fundamental limitation of the algorithm itself, for reasons that will become clear in a moment. We at on stage will improve the algorithm implementation, and we will report on the results in a future paper and update this one accordingly. Technically, the changes are not trivial, and we need to be careful making changes to our research system to ensure that it stays reasonably close to our production system.

The fundamental issue is that we have the derivative of a sum of functions, and the derivative and sum operations commute, leading to the commutative diagram in equation 5.1. This diagram needs some explanation. Firstly, all vector quantities are denoted by bold face, and all scalar quantities by regular face. We have a set of vector-valued function $\mathbf{f}_\nu(\mathbf{x})$ of a vector \mathbf{x} , and the aggregate function \mathbf{F} which is the sum over all the constituent functions $\mathbf{F} = \sum_\nu \mathbf{f}_\nu$. We also have a derivate operator, the *Jacobian operator* \mathbf{J} , which has a matrix-valued result, where the element $\mathbf{J}\mathbf{f}_{ij}$ of \mathbf{J} applied to \mathbf{f} is the partial derivative of the i -th component f^i with respect to the j -the element x_j , as seen in the top right corner in the diagram 5.1. We also have a sum operator Σ that operates either at the vector level if it aggregates function values, or at the matrix level if it aggregates the Jacobian values. The diagram shows two paths to calculate the Jacobian of the aggregate function \mathbf{F} , one in red and one in blue, and the diagram commutes.

$$\begin{array}{ccc}
 \mathbf{f}_\nu(\mathbf{x}) & \xrightarrow{\text{red } J} & \mathbf{J}\mathbf{f}_\nu(\mathbf{x})_{ij} = \frac{\partial f_\nu(\mathbf{x})^i}{\partial x_j} \\
 \Sigma \downarrow & & \downarrow \Sigma \\
 \mathbf{F}_\nu(\mathbf{x}) = \sum_\nu \mathbf{f}_\nu(\mathbf{x}) & \xrightarrow{\text{blue } J} & \mathbf{J}\mathbf{F}_\nu(\mathbf{x})_{ij} = \sum_\nu \mathbf{J}\mathbf{f}_\nu(\mathbf{x})_{ij}
 \end{array} \tag{5.1}$$

The blue path – sum first, then derivative – is easier to implement than the right one. For the blue path, all we have to do is to dispatch the relevant components of the vector

\mathbf{x} that \mathbf{f}_ν needs into the function, and aggregate the result correctly on a coordinate level in the sum function \mathbf{F} . We can for example use dictionaries to create those sparse vector structures which is easy to implement and produces very little overhead. The function \mathbf{F} then has the same interface as the component functions \mathbf{f}_ν , and an unmodified Jacobian algorithm can be fed with the aggregate function \mathbf{F} .

The red path – derivative first, then sum – is somewhat harder to implement because the aggregation for \mathbf{J} happens at the matrix level as opposed to at the vector level, so we need to use different aggregation algorithms for \mathbf{F} and \mathbf{Jf} .

However, the red path has one important advantage that massively reduces the computational effort: all our functions only depend on two variables that for presentational purposes here we call y, z . Also, they only return two values. Therefore, the Jacobian of \mathbf{F} when embedded in the larger matrix looks like in equation 5.2, ie it is mostly zero.

$$\begin{pmatrix} \cdot & \cdot & \cdot & \cdot & \cdot & \cdot & \cdot \\ \cdot & (\partial_y f)_y & \cdot & (\partial_z f)_y & \cdot & \cdot & \cdot \\ \cdot & \cdot & \cdot & \cdot & \cdot & \cdot & \cdot \\ \cdot & (\partial_y f)_z & \cdot & (\partial_z f)_z & \cdot & \cdot & \cdot \\ \cdot & \cdot & \cdot & \cdot & \cdot & \cdot & \cdot \\ \cdot & \cdot & \cdot & \cdot & \cdot & \cdot & \cdot \\ \cdot & \cdot & \cdot & \cdot & \cdot & \cdot & \cdot \\ \cdot & \cdot & \cdot & \cdot & \cdot & \cdot & \cdot \end{pmatrix} \quad (5.2)$$

The consequences of this are important enough to warrant their own proposition:

Proposition 22 (Jacobian complexity). *We assume a system with K tokens and N curves operating on these tokens. Provided all curves only allow exchanging between a uniformly bounded number of tokens, the complexity of calculation their individual Jacobian is $O(1)$ with respect to K , and therefore the overall calculation complexity along the red path (Jacobian first) is $O(N)$. The complexity of calculating the Jacobian*

along the blue path (sum first) however is $O(N \cdot K^2)$.

Proof. If the number of tokens is uniformly bounded, typically 2 or 3 but importantly not depending on K , then the $O(1)$ dependence is obvious. The $O(N)$ is then introduced by the sum, and there is no dependence on K provided the zeroes in the smart vectors are handled intelligently. On the other path however, each calculation of \mathbf{F} is $O(N)$ and it is executed $O(K^2)$ times, thus concluding the proof. ■

In other words, the blue path is a really expensive way of calculating zeroes. In addition to that, the function f^{35} is actually a function of the ratio of its variables only (ie $f(y, z) = \bar{f}(y/z)$). Using the chain rule we obtain the following identities that allow us to cut the number of calculations in half once more:

$$y \partial_y f = -\frac{z}{\partial_z f} = \frac{y}{z} \bar{f}'\left(\frac{y}{z}\right) \quad (5.3)$$

5.4 Scaling the number of tokens

With the mathematics out of the way, we can now discuss the scaling of our implemented algorithm – which follows the blue path in diagram 5.1 – with respect to the number of tokens. For the analysis in this section, we have kept the number of curves at a constant 1,000, which brings us to the region of 1 second calculation time for ECOS/SCS and 10 seconds for Clarabel. The results are presented in figure 5.3 and we make the following observations:

- The marginal price algorithm starts out very well, at about 50ms.
- The performance however deteriorates quite dramatically with the number of tokens as the log/log plot in figure 5.3 shows, and the crossover with ECOS/SCS is at about 100 tokens; our algorithm even seems even on its way to catch up with Clarabel.
- The performance of the convex algorithms is almost flat with ECOS/SCS at about

³⁵A reminder that the function F is the aggregate price response function as defined in 16

1 second, and with Clarabel at about 10 seconds and increasing at the end.

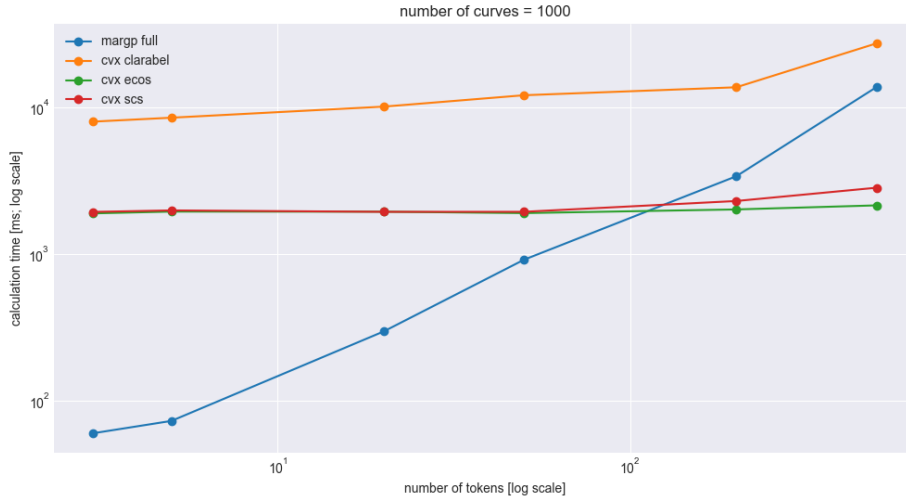


Figure 5.3: *Calculation time versus number of tokens (1,000 curves)*. This chart shows the calculation time for the marginal price algorithm (blue), and the convex Clarabel (orange) and ECOS/SCS (green/red) algorithms as a function of the number of tokens. The chart is on a log/log scale.

This is what we would expect. Additional numbers of tokens for the convex solvers means adding more constraints, but those constraints are covering fewer variables per constraint because the overall number of variables is fixed by the number of curves. ECOS/SCS seem to be mostly oblivious to an increase in token numbers, and even for Clarabel the impact seems muted. However, as shown in proposition 22, the blue path algorithm we are using for the marginal price method is $O(K^2)$ with respect to the number of tokens, and this is what we see in the chart 5.3.

We have not at this stage been able to prove this by implementing the red path algorithm, for the reasons discussed above at the beginning of section 5.3. However, we did profile our current algorithm and measured the cost of the Jacobian calculation as well as that of the other operations, the results of which are shown in figure 5.4. We see that the Jacobian calculation is already starting at about 50 percent of the total processing time for only two tokens, and this increases dramatically with the number of tokens. At 100

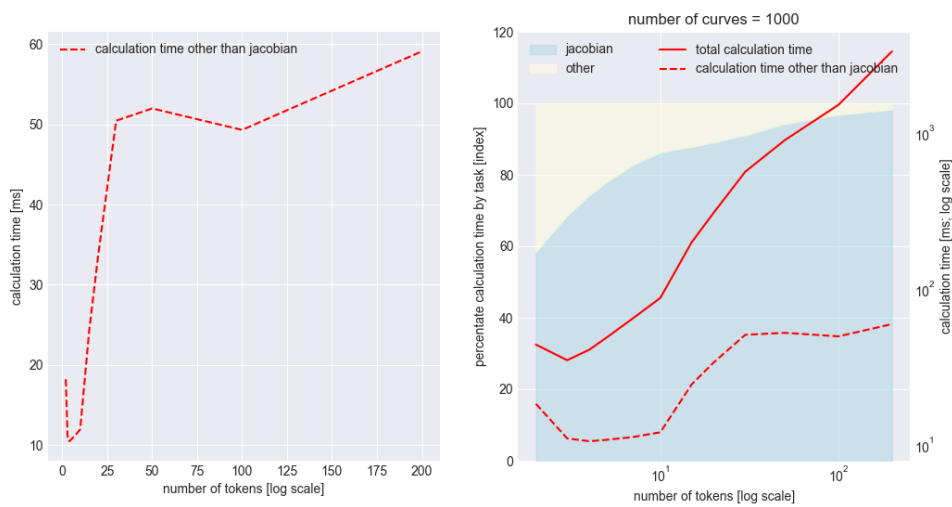


Figure 5.4: *Impact of calculating the Jacobian on the overall performance.* The left hand panel shows the calculation time as function of number of tokens (with 1000 curves) for everything but the calculation of the Jacobian. The right hand panel redraws this on a log/log scale, and adds the calculation time for the Jacobian (solid red). The surface chart in the background shows the percentage of time spent on the Jacobian calculation (linear scale).

tokens, virtually all processing time is consumed by the the calculation of the Jacobian. We can see this by looking at the surface plot in the left panel, and also by the fact that the time requirements for the non-Jacobian calculations displayed in the left hand panel become quickly flat at about 50ms over all 1,000 curves, regardless of the number of tokens.

6 Conclusion

This concludes the first paper describing the mathematics and algorithms underlying our FastLane Arbitrage bot [15]. This bot is monitoring various chains, and specifically the DEXes and Carbon DeFi deployments thereon, and is looking for arbitrage opportunities there (ie it is looking for trades that allow it to make a profit without taking any risk). This first paper is focussing on the newly developed *marginal price framework* for identifying all arbitrage opportunities in a specific market or submarket.

The core of this paper is section 3 where we have described the the *marginal price optimization algorithm*³⁶ for arbitrage and optimal routing and where we have shown in theorem 19 that it is outcome-equivalent to the convex optimization problem developed in [6, 7, 12] and described in section 2. This algorithm dramatically simplifies the optimization problem by only searching on the optimal surface described by the marginal prices between the tokens in the system. This reduces the number of variables from *two per curve* to *one per token*³⁷, and converts the optimization problem into an often better conditioned root finding problem.

We discussed in section 5 that our algorithm outperforms convex optimization³⁸ by a factor of 75x on ECOS/SCS solvers, and a factor of 200x for CVXPY’s new standard solver Clarabel. Also, whilst our algorithm still experiences convergence issues in markets

³⁶We refer to it as “optimization” for historical reasons because of its relationship to convex optimization; technically however it is a root finding algorithm

³⁷In fact, number of tokens minus one

³⁸Specifically, the convex optimization algorithm in token space proposed first in [6]; we believe our algorithm still outperforms the conjugate algorithm proposed in [12] but as its publication of this algorithm coincided with the finalization of our arbitrage bot we never tried to implement it

that are dominated by certain configurations of levered curves, it is significantly more robust in this respect, and the reasons for divergence are well understood.

We have presented two different implementations of the marginal price algorithm, the *pair optimizer* based on the bisection algorithm, described in section 4.1, and the *full optimizer* that is based on the Newton-Raphson / gradient descent algorithm described in section 4.2. As the name implies, the pair optimizer only work on pairs, and we have found that whilst it is slower than the full optimizer by a factor of up to 10x, it is more robust – in fact it always converges, regardless of market conditions. Therefore, the decision which optimizer to use for pairs can be hard³⁹, depending whether one values resource use and latency or robustness more.

This paper only covered part of the technology underlying the FastLane Arbitrage bot. Notably what is missing is

- *transaction decomposition* where we limit the number of curves involved in an arbitrage transaction to maximise the chances that an arbitrage transaction will go through, and
- *transaction linearization* where we ensure that arbitrages can be executed in a linear manner in situations where flashloans are available only for certain tokens, and where the arbitrageurs only as access to limited token amounts.token holdings are limited.

We also developed another algorithm – the `_Graph Mode_` – that uses a completely different approach to identifying arbitrage opportunities, and that does not suffer from the same convergence issues as the marginal price algorithm. It however displays other issues, notably around scaling, that we are still working through. Ultimately we will probably settle on a *horse-for-courses* approach where both algorithms are used in their respective sphere.

³⁹One may also consider combined applications that start with the full optimizer on pairs, and escalate cases of non-convergence to the pair optimizer

All of the above are subject to forthcoming papers that we currently have in preparation, and that we will publish in due course.

References

- [1] Stephen Abbott. *Understanding Analysis*. Springer, New York, 2nd edition, 2015.
- [2] Hayden Adams. Uniswap: A Constant Product Market Maker for decentralized finance. Technical report, Uniswap Labs, November 2018. Whitepaper.
- [3] Hayden Adams. Uniswap whitepaper [work in progress]. Technical report, 2018.
- [4] Hayden Adams, Noah Zinsmeister, and Dan Robinson. Uniswap v2 core. Technical report, Uniswap Labs, March 2020. Whitepaper.
- [5] Hayden Adams, Noah Zinsmeister, Dan Robinson, Moody Salem, River Keefer, and Alex Martinelli. Uniswap v3 core. Technical report, Uniswap Labs, March 2021. Whitepaper.
- [6] Guillermo Angeris, Akshay Agrawal, Alex Evans, Tarun Chitra, and Stephen Boyd. Constant Function Market Makers: Multi-asset trades via convex optimization, 2021.
- [7] Guillermo Angeris, Tarun Chitra, Alex Evans, and Stephen Boyd. Optimal routing for Constant Function Market Makers, 2022.
- [8] CVXPY authors. CVXPY. <https://www.cvxpy.org/>.
- [9] Stephen Boyd and Lieven Vandenbergh. *Convex Optimization*. Cambridge University Press, Cambridge, UK, 2004.
- [10] Wikipedia contributors. Radome (Wikipedia). <https://en.wikipedia.org/wiki/Radome>, 2024. Accessed: 2024-10-02.
- [11] George B Dantzig and Mukund N Thapa. *Linear Programming 1: Introduction*. Springer Series in Operations Research and Financial Engineering. Springer, New York, NY, 1997.
- [12] Theo Diamandis, Max Resnick, Tarun Chitra, and Guillermo Angeris. An efficient algorithm for optimal routing through Constant Function Market Makers, 2023.

- [13] Steven Diamond and Stephen Boyd. CVXPY: A Python-embedded modeling language for convex optimization. *Journal of Machine Learning Research*, 17(83):1–5, 2016.
- [14] Daniel Engel and Maurice Herlihy. Composing networks of Automated Market Makers. In *Proceedings of the 3rd ACM Conference on Advances in Financial Technologies*, AFT '21. ACM, September 2021.
- [15] Bprotocol Foundation. ArbFastLane. <https://bancor.network/arbfastlane>.
- [16] Bprotocol Foundation. ArbFastLane repository. <https://github.com/bancorprotocol/fastlane-bot>.
- [17] Bprotocol Foundation. Bancor protocol. <https://bancor.network/>.
- [18] Bprotocol Foundation. Carbon protocol. <https://carbondefi.xyz/>.
- [19] Uniswap Foundation. Uniswap protocol. <https://uniswap.org/>.
- [20] Herbert Goldstein, Charles Poole, and John Safko. *Classical Mechanics*. Addison-Wesley, San Francisco, 3rd edition, 2002.
- [21] Eyal Hertzog, Guy Ben Artzi, Galia Benartzi, and Yehuda Levi. Methods for exchanging and evaluating virtual currency [US Patent 12045807B2], 2024.
- [22] Eyal Hertzog, Guy Benartzi, and Galia Benartzi. Bancor Protocol: Continuous liquidity and asynchronous price discovery for tokens through their smart contracts; aka "Smart Tokens". Technical report, Bprotocol Foundation, 2017. Draft Version 0.99.
- [23] Eyal Hertzog, Yehuda Levi, Barak Manos, Asaf Shachaf, and Guy Ben Artzi. Smart contract of a blockchain for management of cryptocurrencies [US Patent 20240119444A1], 2024.
- [24] John C Hull. *Options, futures, and other derivative securities*. Prentice Hall, 2 edition, 1993.

- [25] Stefan Loesch. The quantitative finance aspects of Automated Market Makers in DeFi, 2022.
- [26] Stefan Loesch, Nate Hindman, Mark Bentley Richardson, and Nicholas Welch. Impermanent Loss in Uniswap v3, 2021.
- [27] Stefan Loesch and Mark Bentley Richardson. Decomposing arbitrage transaction, forthcoming.
- [28] Fernando Martinelli and Nikolai Mushegian. A non-custodial portfolio manager, liquidity provider, and price sensor [Balancer Whitepaper]. Technical report, September 2019. Whitepaper.
- [29] J. A. Nelder and R. Mead. A Simplex Method for Function Minimization. *The Computer Journal*, 7(4):308–313, 01 1965.
- [30] NumPy authors. NumPy. <https://numpy.org/>.
- [31] Mark Bentley Richardson and Stefan Loesch. Carbon: A decentralized protocol for asymmetric liquidity and trading. Technical report, Carbon Protocol, November 2022. Last updated: 7 Jan 2023.
- [32] Mark Bentley Richardson and Stefan Loesch. Carbon litepaper: A decentralized protocol for asymmetric liquidity and trading. Technical report, Carbon Protocol, November 2022. Litepaper.
- [33] Mark Bentley Richardson and Stefan Loesch. DeFi’s concentrated liquidity from scratch, 2024.
- [34] Mark Bentley Richardson, Stefan Loesch, Barak Manos, and Asaf Shachaf. Customizable cryptocurrency trading [WO Patent 2024084480A1], 2024.

Appendix

A The Radome Optimization Problem

A “radome” [10] is a structure that protects a radar antenna from the elements, and typically has the geometry shown in figure A.1. It also provides an excellent example for a class of convex optimization problems, referred to herein as the “*radome optimization problems*”.

Definition (Radome Optimization). *The “Radome Optimization Problems” are a class of convex optimization problems that arise when searching for an optimal point on a radome. They differ in two aspects, firstly the exact nature of the shape of the radome, and secondly the objective function that is to be optimized.*

*In terms of radome shapes we consider the following types (a) the **balloon type**, a smooth surface that is convex in all directions (b) the **planar type**, a collection of flat surfaces that is convex in all directions, like shown in figure A.1 and (c) the **mixed type**, a “mostly smooth” surface that can be thought of as replacing the flat surfaces in the planar type with convex surfaces, in a manner that retains the vertices and edges of the planar type and overall convexity.*

*In terms of objective functions we consider (1) a **linear** function like “height” or “distance to the sun”, or (2) a **non-linear** one like “distance to a nearby point”.*

The problems A1 and A2 are traditional smooth optimization problems that can be solved with Lagrange multipliers [20]: at the optimal point, the gradient of the constraint must be equal to the gradient of the objective function, the latter being constant $(0, 0, 1)$ in case of the “height” function in (1) and a vector pointing in the direction of the sun in the general linear case. In case (2) the gradient is orthogonal to the usual equidistance surfaces around the target point.

If we assume the radome is the unit sphere then the solution of A1 in the height case is the north pole, and more generally $\mathbf{x}/\|\mathbf{x}\|$ where \mathbf{x} is a vector pointing in the direction

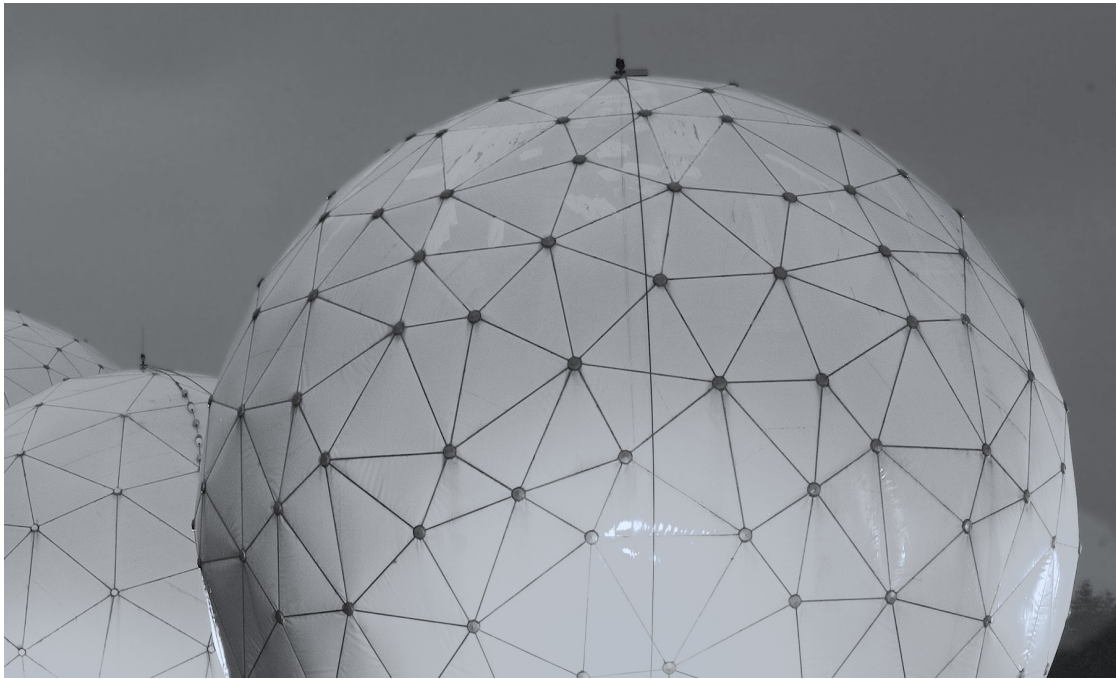


Figure A.1: *Example for a radome.* Example for a radar dome (“radome”), a structure that consists of flat or near flat segments touching one another along non-smooth connector lines (image credit Wikipedia)

of the sun.

The planar type radome – the usual form as depicted in figure A.1 – is an example for a set of linear constraints: for each of the faces $\nu = 1 \dots M$ we have a linear condition on the points \mathbf{x} inside that radome that reads

$$\mathbf{n}_\nu \cdot \mathbf{x} \leq \mathbf{n}_\nu \cdot \mathbf{x}_\nu \tag{A.1}$$

where \mathbf{n}_ν is the normal vector of the face ν , and \mathbf{x}_ν is any point on that face. We note that the normal vector \mathbf{n}_ν is the equivalent of the gradient of the constraint in the smooth case. Therefore the Lagrange condition above cannot usually be strictly satisfied⁴⁰. In case we have linear constraint here we arrive at the well-known *linear-programming* problem as described in many text books (eg [11]). In this case the solution is almost always⁴¹ at a vertex of the radome, which it can be found, for example, using a *simplex algorithms*.

The interesting cases – and most relevant for us – are B2 and C1; B2 because it is the most intuitive and C1 because it most closely relates to the actual problem we are solving, which has a linear objective function on a mixed-type-constraint hyper-surface.

Starting with B2, the solution has two steps: we need to find the face that is closest to the target point, and on the face we need to find the actual closest point. The algorithm for finding the optimal face is similar to the simplex algorithm in linear programming, except that we have a duality where faces now play the roles of vertices and vice versa. Once we have identified the face we can then use a gradient algorithm to find the optimal point on that face⁴².

In case of C1 and C2, the constraint itself is neither linear nor entirely smooth. Depend-

⁴⁰To formalize this statement we could introduce a measure on the space of gradients that is uniform on the unit sphere and when the sphere is deformed into a planar structure we find that all mass will be in the vertices in the sense that faces and edges are of measure zero

⁴¹In the sense of the measure introduced in the previous footnote

⁴²In case of a simple metric, we could of course do this part of the calculation analytically, but for didactical reasons we assume that we do not have this shortcut available to us

ing on the convexity of the faces, there is now a finite chance⁴³ of the solution being an “*interior solution*” (on one of the faces) and a finite chance of it being a “*corner solution*” (on a vertex or edge). Again we may use a simplex-type algorithm to identify the optimal face, and on the face we may use a gradient descent to lead us to the optimal point. Importantly, we cannot simply start with a gradient descent before we have identified the correct face because due to the non-smoothness of the constraint function the local geometry is not a good guide to the global geometry of the problem.

B The Repatriation Problem

Here we discuss the *repatriation problem* referred to in section 3.3 in more detail. High level, the issue is when an arbitrage opportunity exists, but the profits cannot be extracted because there does not exist sufficient capacity to trade into the chosen target token. For example, consider the following set of curves providing the arbitrage:

- Buy/sell USDC for USDT at 0.99 USDT per USDC (1m USDT capacity)
- Sell/buy USDT for USDC at 1.01 USDT per USDC (significantly larger capacity)

Assuming those curves are infinitesimally thin, one possible trade here is to start with $1m$ USDT, sell them for $1.01m$ USDC on the first curve, and to sell those against USDC for $1.02m$ USDT, yielding a profit of $20k$ USDT. Alternatively one can start with $0.99m$ USDC, sell them for $1m$ USDT on the second curve, and sell those for $1.01m$ USDC. Again, the profit is $20k$ USDC. Using thicker curves⁴⁴ will somewhat blunt that opportunity and for the purpose of the argument we assume that we can make USDx $15k$ in profit in either direction.

⁴³The term “chance” is again to be understood in terms of the measure on the gradients introduced above; here, because the faces have a non-zero convexity, there is a non-zero mass of the distribution of gradients on the faces, so not all of the mass is concentrated in the vertices

⁴⁴The MPF algorithms will not be able to deal with infinitesimally thin curves to accurately determine trading volumes, so in practice we will need to regularize the curves by imposing a minimum width; the SOF algorithm operates on amounts rather than prices so in principle would be able to handle it; however we have found in practice that the SOF algorithms available to us would perform worse than our MPF algorithm

In either the convex optimization formulation (“COF”) according to definition 3 or the marginal price formulation according to definition 18 we need to define a target token in which to extract the profits. If it is either USDC or USDT both will find the same solution – a target token of USDT will yield the first of the solutions above, and a target token of USDC will yield the second one.

We now assume that the target token is WETH, and we will consider a number of different cases.

High capacity curve. The baseline positive case is that there is a high capacity curve linking USDx to WETH. In this case both algorithms will converge nicely, the MPF one by choosing the price on the WETH curve that absorbs the 15k profit, and the COF that works on quantities rather than prices by pushing those 15k through the WETH curve at whatever price that yields.

Low capacity unlevered curve. We now consider any unlevered curve linking USDx to WETH. The magic of unlevered curves is that they can absorb any token amounts – the only question is at which price. Fundamentally this is not different from the *high capacity curve* case above: both algorithms will converge, one by pushing the 15k USDx into the curve, the other one by finding a price point at which the 15k USDx can be absorbed. The difference to the high capacity case is only that the curve is restricted by its WETH token balance in what it can release – if it holds 1 WETH then max output will be (below but possibly close to) 1 WETH; if it holds 0.1 WETH it will be 0.1 WETH and so on. In other words: the algorithms will converge⁴⁵, albeit possibly to a solution that is not particularly advantageous.

Limited capacity levered curve. We now consider a levered curve that is linking USDx into WETH. The key difference between this and the *low capacity unlevered curve* case is that because prices are bounded there is a maximum amount of USDx that this curve can absorb. Once it has dispensed all its WETH, and reached the, from the trader’s perspective, worst possible price in the range covered, it will simply stop

⁴⁵Unless the MPF algorithm has a price cutoff that is being hit

trading. The COF algorithm should converge: provided the solver can deal with the boundary condition it will understand the maximum amount that can be repatriated and will adjust the trade amounts through the USDx curves accordingly. The MPF algorithm will do the same, provided that (a) it can adjust the prices on the USDx curves sufficiently finely to ensure the profit matches the capacity on the curve, and (b) the price adjustment of the USDx/WETH curve is done in a way that either it does not overshoot the boundary, or the algorithm can deal with overshooting into the no-man’s land beyond the curve without failing.

No curve. Finally we assume that there are no curves linking either of the USDx tokens to WETH, directly or indirectly. How will this manifest itself in the two cases? In the SOF it will depend on the solver. Ultimately, because there is no path into WETH none of the operations the optimization algorithm performs on the USDx curves will impact that target function. Therefore, ultimately it will fail because whatever it does, the target function will remain unaffected. In the MPF case we can see this even more clearly. The Jacobian defined in equation D.6 will be singular because all derivatives between USDx and WETH will be zero⁴⁶. This in turn means that the update rule in equation D.9 will fail⁴⁷ and the algorithm will run into the max iteration limit without being able to fulfil the solver condition of $\Delta\text{USDC} = 0$ and $\Delta\text{USDT} = 0$.

In summary – both algorithms, if sufficiently well done, converge to the same result under the repatriation problem. There will be no convergence in case no repatriation is possible because there are no curves, and if repatriation is limited then they will restrict the amount of USDx arbitrage performed.

⁴⁶The “no indirect connections” condition here is important; if there are trade opportunities between USDx and WETH that go via other tokens then the Jacobian will not be singular

⁴⁷Note that it will fail despite the modified update rule that ignore the null space when trying to invert the Jacobian, the issue being that the null space is the one connecting USDx and WETH

C The Multiple Solutions Problem

Here we discuss the *multiple solutions problem* referred to in section 3.3 in more detail. High level the issue is that there could be multiple solutions to the optimization problem that perform equally well in terms of arbitrage profits, but they result in different trading instructions. The archetypical example is buy-low-sell-high where there are multiple options to trade into at the same conditions and where the volume is limited on the other side. Consider the following set of three curves, all with a capacity of 1m USDT:

- Curve A: Buy/sell USDC for USDT at 0.99 USDT per USDC
- Curves B1, B2: Buy/sell USDC for USDT at 1.01 USDT per USDC⁴⁸

The trade is buying 1m USDC on curve A at 0.99 USDT and selling it into B1 or B2 or any combination thereof at 1.01 USDT, for a profit of 20k USDT. The multiple solutions come from the fact that, provided there is no slippage, there is no difference selling into B1, B2 or into any combination thereof that has the right capacity.

The point about no slippage is important here. If there were slippage on the curves, there would be a unique solution to the optimization problem: partitioning the trade so that the post-slippage marginal prices are the same across all curves. This issue only arises because the marginal prices do not move with volume.

The algorithm under the convex optimization framework (“COF”) operates on quantities, and moving quantities between B1 and B2 does not impact the target function. Any well designed algorithm will not stumble over this, and the chosen partition will depend on details of the algorithm and starting conditions. The algorithm under the marginal price framework (“MPF”) however operates on prices instead of volumes – the latter are implied. Therefore the MPF algo cannot operate on no-slippage curves, and in our implementation of the algorithm we regularize the curves by enforcing a certain minimum width. Therefore the MPF algorithm will always converge to a unique post-

⁴⁸The curves B1, B2 could be composite curves trading through one or multiple other tokens, and there could be more than two curves, none of which would substantially change the argument

regularization solution, equalizing the marginal prices on all curves and distributing the trade volume accordingly.

D Numerical Methods

In this appendix, we discuss the bisection and Newton-Raphson methods, and how they can be used for finding minima and maxima and roots.

D.1 Bisection Method

The bisection method is a root-finding method for one-dimensional functions that has very interesting properties. Notably, it is very robust in that it is guaranteed to converge (depending on the convergence criteria chosen) on a very wide range of functions, including those where roots do not really exist.

D.1.1 Finding roots

The algorithm is very simple: given function $f(x)$ and a *bracketing* interval $[a, b]$ such that $f(a)$ and $f(b)$ are of different sign, we can find a root of any continuous function by repeatedly bisecting the interval, checking the sign of the mid point, and moving the boundary of the interval that has the same sign as the mid point to the mid point.

This algorithm yields a sequence (a_i, b_i) of intervals such that $f(a_i)$ and $f(b_i)$ have different signs, and the length of the interval $|b_i - a_i|$ halves at every step, and therefore converges to zero. Because of the intermediate value proposition, we know that if f is continuous, there is (at least) one root in the interval $[a_i, b_i]$, and therefore the location of the root can be approximated to arbitrary precision.

In the figure D.1 we are providing a number of example of functions and we briefly discuss how the bisection method can be used to find the roots. We start with the left hand panel where we have continuous functions, and we assume that the starting interval $[a, b]$ is such that $f(a)$ and $f(b)$ have different signs, but not necessarily symmetric around the origin. For the highly regular “*softsign*” function, we can see that the bisection method will always converges to the root at $x = 0$. Moreover, because the derivative is uniformly bounded in the sense of equation D.1, we can propagate the error on the x axis to the y axis, meaning that we not only know that position of the root with a certain

precision $\varepsilon \simeq b_i - a_i$, but we also know that the error on the y axis is approximately bounded by $c\varepsilon$.

$$\exists c \forall x \in [a, b] : |f'(x)| \leq c \quad (\text{D.1})$$

With the trigonometric “*sine*” function, we can see that the bisection method will converge to a root as well, provided we start with an interval that has opposing signs. However, the function has multiple roots, and to which of them we converge will depend on the choice of the starting interval.

Finally we have the “*root*” function $f(x) = \sqrt[3]{x}$. This function has a root at $x = 0$, but at this point the derivative is unbounded. Therefore the error on the y axis can be quite big, even if the convergence on the x axis is advanced.

In the right hand panel of the figure D.1 we have some more pathological, specifically discontinuous functions. Firstly, to make the obvious point: two out of the three functions do not have roots, in the sense that $f(x) = 0$. However, they have “*root locations*” x_0 where they change sign:

$$\exists x_0, \varepsilon, s \forall x^- \in (x_0 - \varepsilon, x_0) \forall x^+ \in (x_0, x_0 + \varepsilon) : sf(x^+) \geq 0, sf(x^-) \leq 0 \quad (\text{D.2})$$

Note that not all functions have this property. For example, consider $f(x) = \sin(1/x)$ with $f(0) = 0$ around $x = 0$. This function has an infinite number of roots that are dense around $x = 0$, so there is no ε that could separate them. However, if the functions we consider are continuous except for a finite number of points in every finite interval, that above equation will apply and distinct roots locations can be identified and found with the bisection method. The value on that location of course may be undefined, in the sense that the left and right limits do not coincide (and neither of them may be zero) in any case (the “*sign*” function), or those limits do not even exist (the “*inverse*” function $f(x) = 1/x$). However, especially in the “finite jump” case we note that we

can always regularize the function (eg by convolution), leading to something akin to the “*softsign*” function, which is C^∞ with bounded derivative (for every fixed value of the regularization parameter), and which matches finite-size functions reasonably well. As previously mentioned, this case is particularly important to us, because limit orders correspond to discontinuous functions. To make them continuous, even differentiable, we regularize these orders by converting them into very narrow range orders.

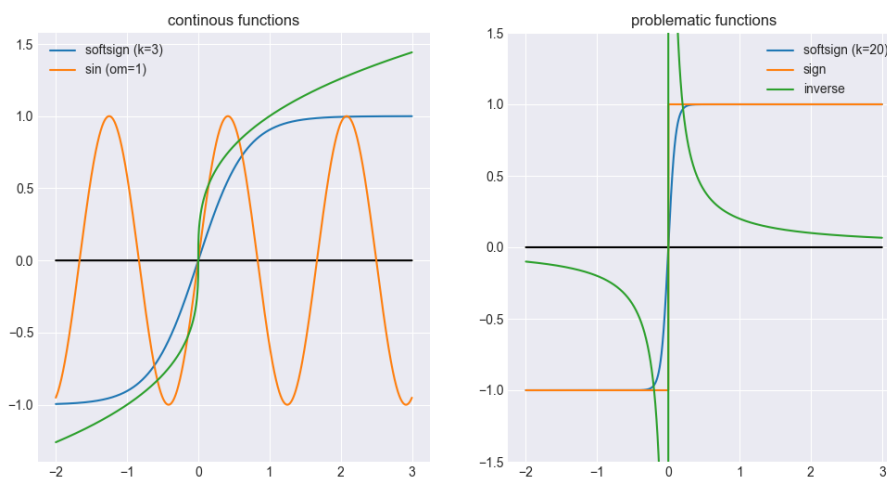


Figure D.1: *Example functions for root search.* Both panels show functions discussed in the text for the performance of the root search algorithm on them. The left hand panel has benign functions that have one or multiple regular roots. The right hand panel shows functions that have a root location but either very badly conditioned root (blue), or not roots at all, with a finite jump (orange) or an infinite one (green).

D.1.2 Finding minima and maxima

The bisection method can also be used to find (interior) minima and maxima of functions by using the fact that the derivative of a function is zero and changes sign at those points. In other words – if we are looking for minima or maxima we can use the bisection method to find the roots of the derivative of the function. The derivative can be calculated either analytically, or numerically for example using the *finite difference formula* D.3 for some small value of h :

$$f'(x) \simeq \frac{f(x+h) - f(x-h)}{2h} \tag{D.3}$$

Again, this algorithm is very robust. Specifically, we again consider the case of a non-differentiable function like the one in figure 1.3. As we can see in the right hand panel, the derivative is a step function that is constant between the steps (ie it locally looks like the sign function in figure D.1). We have seen that those functions can be regularized (eg using a convolution method), yielding functions similar to the softsign function in the same figure. This function is differentiable and therefore the bisection method will converge to the correct root of the regularized function. However, we actually do not have to regularize the function for the algorithm to converge. As discussed above it will converge, on the x axis, to the root location as defined above. The error is more benign than in the root finding case. As we are looking for a maximum or minimum, by design the area around the root is somewhat flat, therefore in practical applications the error on the y axis is typically small. However, it must be stressed that the term “in practical applications” is an important caveat here. In particular we can imagine a very spiky function – think Dirac Delta. For example, if we look at a Gaussian kernel function as defined in equation 1.6 and we take a very big value of λ – which is a popular choice for a Dirac-Delta-like C^∞ function – then the bisection method will find the location of the spike, but it may not be that good at estimating its exact height.

D.1.3 Convergence

To build on our previous discussions we now briefly discuss the convergence properties of the algorithm. We only discuss the root finding case here, but the discussion can be easily extended to the minima and maxima case by replacing the function with its derivative.

Firstly, we know that, provided the start conditions are fulfilled, the algorithm always converges “*exponentially*” on the x-axis, and we know exactly the speed of convergence: after n steps, the size of the interval will be 2^{-n} of the original interval size. See figure

D.2.

Convergence on the y-axis depends on the type of function we are looking at.

Differentiable with bounded derivative everywhere. If the function has a bounded derivative in the initial interval (or any interval subsequently chosen by the algorithm) then convergence on the y-axis is equally exponential in nature. This is the case we will mostly encounter in our problem set, and the bisection method is an excellent and reliable method to find roots in this case.

An important sub case of this is where the function is **differentiable twice everywhere**, which implies that in any compact interval – and we only care about those for numerical applications because we need to choose our initial $[a, b]$ – the derivative is bounded, which means the above condition applies.

For the next condition we introduce the notion of separated points a variation of which we have already seen in equation D.2: a set of points $\{x_i\}$ is separated if there exists an ε so that for all $i \neq j$ we have $|x_i - x_j| > \varepsilon$.

Continuously differentiable everywhere except for separated points. The next case we consider is the case where the function is differentiable and the derivative is continuous everywhere in the initial interval, except for a set of separated points. The interesting point here of course is if the root is amongst those points as, otherwise, we will eventually find an interval where we are essentially back in the first case.

So, if the root location is one of those points, the algorithm will converge to it, as defined in equation D.2, but we can't make any predictions about the error on the y-axis. For example, look at the right hand panel of figure D.1 for examples of such functions. For example, if we use the sign function, unless we by chance hit the root exactly, the value at the mid point will either be 1 or -1. Even worse is the case of the inverse function $1/x$ where the mid point of the converged interval will be the larger in absolute value the smaller the interval is, on top of the uncertainty around its sign.

In other words – in this case, whilst we can be certain about convergence on the x-axis,

convergence on the y-axis is undetermined, and in the worst case the longer we run the algorithm, the further the value diverges from zero.

There are more pathological cases of functions that we can consider here. For example, we can have a function with an infinite number of roots in any finite interval containing a specific point (eg, the aforementioned $\sin(1/x)$ around zero). In this case, the algorithm will still converge on the x-axis but we do not know where to. Whilst this case is interesting from a mathematical point of view, it is not relevant for our problem set as we will only encounter functions of the first two types in our problem set.

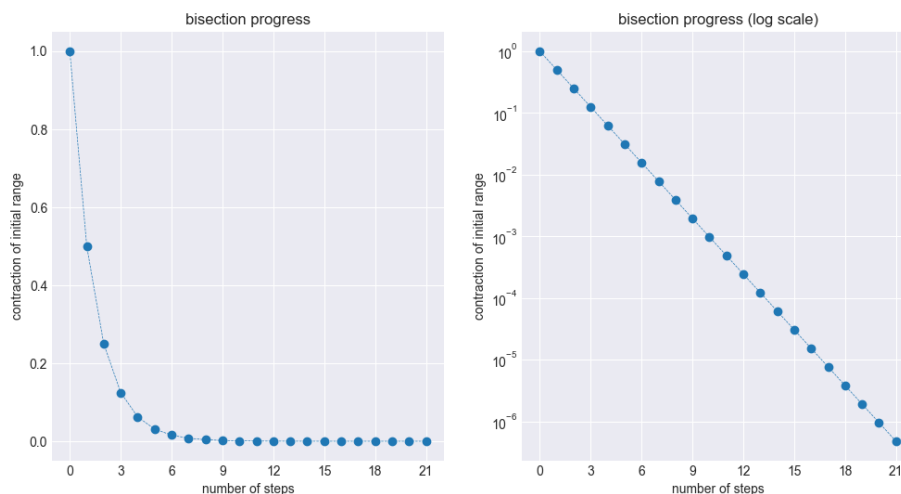


Figure D.2: *Bisection progress over time*. Both panels show how the size of the bisection bracket contracts with number of steps, compared to the initial size of the bracket. The left hand panel is on a linear scale, the right hand panel is on a log scale.

D.1.4 Higher dimensions

The bisection method is hard to extend to higher dimension because the geometry of the problem is more complex, and because the intermediate value proposition no longer applies. To understand this, we want to look at the following two dimensional problem

$$f(\mathbf{x}) = \begin{bmatrix} f(x) \\ f(y) \end{bmatrix} = \begin{bmatrix} x + y - b \\ x^2 + y^2 - 1 \end{bmatrix} = \begin{bmatrix} 0 \\ 0 \end{bmatrix} \quad (\text{D.4})$$

that depends on a parameter b . Note that of course in two dimension we not only have two variables but also two functions, and we are looking joint root $f(\mathbf{x}) = \mathbf{0}$. We have drawn the level sets for two different parameter values of b in the figure D.3. In both panels we see the circle of radius one that is the level set of the second function. In the left panel we also see the line $y = 2 - x$, whilst in the right panel we see the line $y = 1 - x$.

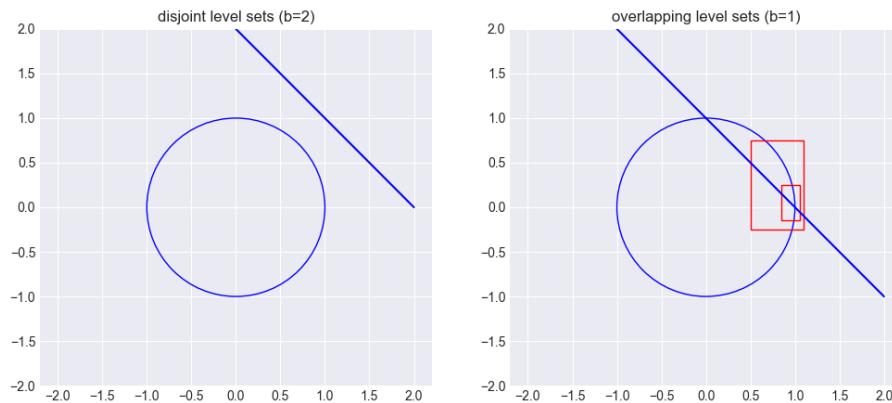


Figure D.3: *Attempting multi-dimensional bracketing.* Both panels show the level sets $f_i(\mathbf{x}) = 0$ ($i = 0, 1$) for the two components of vector valued function \mathbf{f} . In the left panel, those level sets do not intersect, so the equation $\mathbf{f}(\mathbf{x}) = \mathbf{0}$ does not have a solution. On the right hand panel, the level sets intersect so there are solutions. The red rectangles represent an attempt at two dimensional bracketing discussed in the text.

Firstly we note that the left panel does not have a solution to the problem as the two level sets do not intersect and therefore there is not joint root. However, the right panel does have two solutions, at the intersection points of the circle and the line.

We recall that for a bisection method we need a change of sign, and we note that above

(below) the line and outside (inside) the circle sign of the respective function is positive (negative). We note that only on the right panel we can identify a (hyper)rectangle where all possible signatures are present: if we start from the bottom left and go clockwise we have $(-, -)$, $(+, -)$, $(+, +)$, $(-, +)$. We also note that there is a root in this space. This is not by chance. If we can contract the rectangle to zero without changing the border signatures (as indicated with the smaller rectangle) we will eventually converge against a root location. However, in this process we encounter a number of problems

- How do we know that there is a (joint) root? In high dimensions this problem is much harder to solve than in one dimension.
- Relatedly, how do we identify the hyper-rectangle that satisfies the correct signature conditions at the boundary?
- Finally, if we have such rectangle, how do contract it without violating the boundary conditions?

None of those problems are unsolvable. However, they are hard enough that bisection in higher dimensions is not a popular method for generic problems, and we will only consider it in one dimension.

D.2 Newton-Raphson Method

The Newton-Raphson method (also named “Gradient Descent”) uses the first derivative (“gradient”, in higher dimensions) of a function to find its roots. A worked example is provided in the figure D.4. Here the algorithm starts at a point $x_0 \simeq 1$ (1a). This point is transported along the orange tangent line to the point (1b) where that tangent line intersects the x axis. Point (2a) has the same x coordinate as (1b), and the process is repeated. We see that (4b) is already very close to the root, which is a general result of gradient descent methods. On benign functions they converge very quickly to the root – and of malignant functions they may not converge at all, but we will discuss this in more detail below.

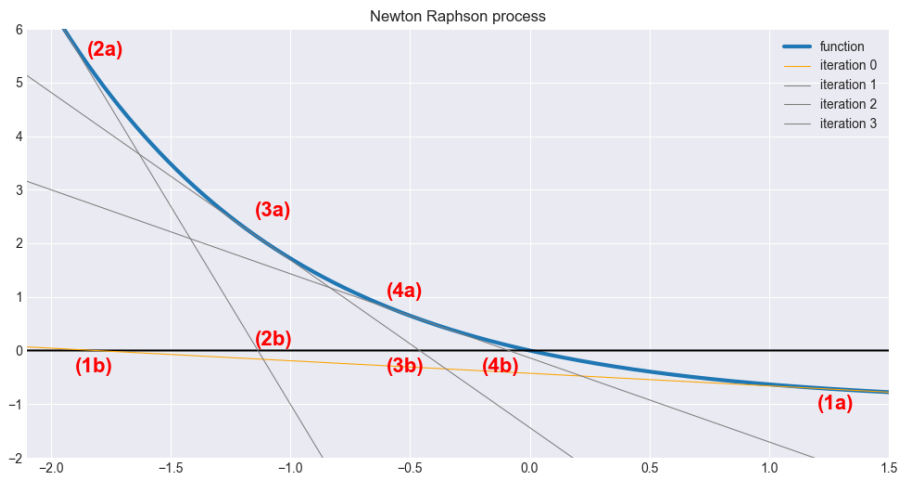


Figure D.4: *Newton-Raphson worked example.* The above figure shows the Newton-Raphson method in action. The blue line represents the function whose root is to be determined. The algorithm starts at point (1a) and gets moved along the orange tangent to (1b). The process then repeats from (2a) which is the same x coordinate as (1b) via the black tangents up to the point (4b) that is in our example judged sufficiently close to being a root.

D.2.1 Convergence

We now want to discuss the convergence properties of the Newton-Raphson method. The first thing to note is that on a linear function it will converge in a single step, by design. The issues are generally introduced by convexity. A few observations:

- If the convexity is directed “towards” the x axis (ie what happens in figure D.4 in the area where $f(x) > 0$), and the root exists, convergence is guaranteed and swift.
- If the convexity is directed “away” from the x axis (ie what happens in figure D.4 in the area where $f(x) < 0$), and the root exists, then the algorithm will move to the other side of the root.
- If convexity has the same sign across the entire real axis, and the root exists, the algorithm will converge, because either the convexity is directed towards the x axis in the region of interest, or the first step transports the algorithm to the other side of the root into a region where the convexity is directed towards the x axis.

Now we look at a few things that can go wrong. Firstly, we look at what happens if there is no root to be found. This case is in figure D.5 in the top-left panel (a). We start at point (1a) and because there is no root, step (2a) overshoots to the other side of the minimum. Step (3a) then brings us back very close to the minimum, and because the function there is very flat, step (4a) brings us very far to the left. In this case, the algorithm will enter an infinite cycle that will only break if either we hit exactly the minimum where $f'(x) = 0$ and we get a division by zero, or we leave the domain where the function has been defined, or we hit a numerical limit. Note the top-right panel which is the same function, except that it (just) has a root. There, the convergence is just fine.

What we have just seen is that the algorithm does not converge if there is no solution that can be found. This can be a nuisance sometimes, but arguably it is not a major issue – after all there is no root to be found, and non-convergence is a good albeit possibly

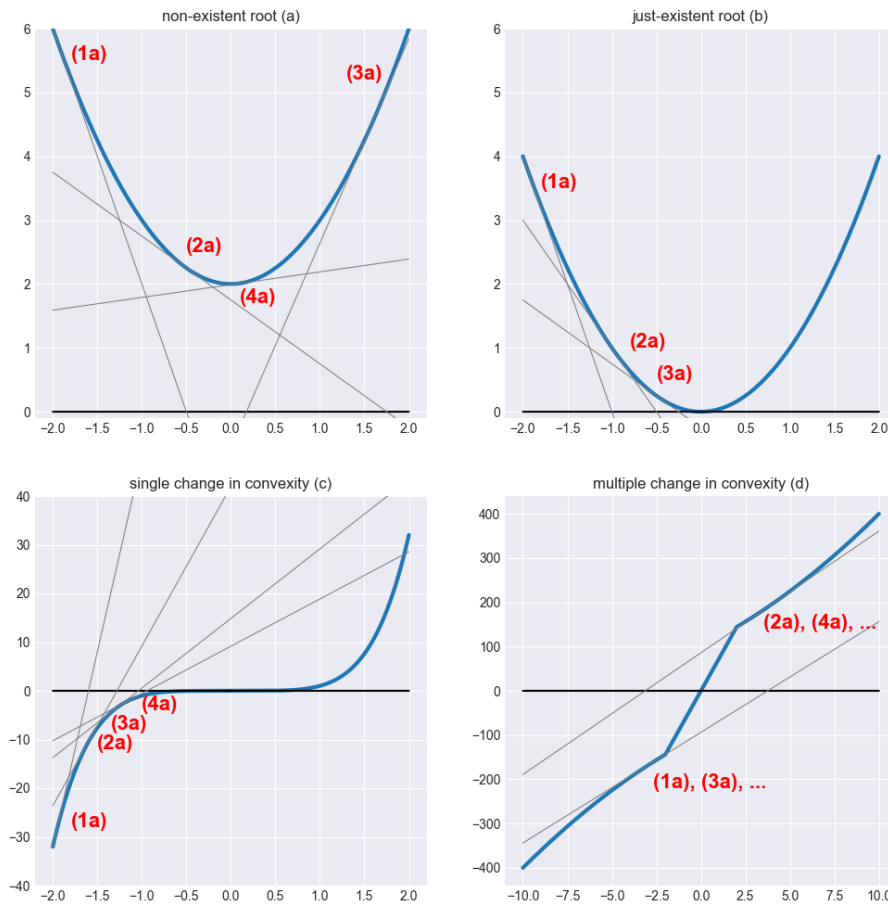


Figure D.5: *Examples of Newton-Raphson with potentially problematic convergence.* Those four panels show how the Newton Raphson algorithm performs on some problematic functions. The labels are like in figure D.4 except we omit the (b) labels. The top left panel has no root, and the algorithm enters an infinite cycle. The top right panel as a comparison shows the same function with a root. There convergence is fine. The bottom left panel shows a function with a single inflection point where convergence is fine. The bottom right panel shows a function with two inflection points that has a perfectly well conditioned root, but where the algorithm enters an infinite cycle because of the badly chosen starting point.

expensive indicator of that. The other case we look at is if there is a change in convexity. As the bottom-left panel (c) shows, this can be alright if there is a single inflection point. However, as the bottom-right panel (d) shows, multiple inflection points, especially with very high or even infinite convexity values, can lead the algorithm into an infinite cycle. This is particularly vexing as the function is generally very well behaved, and had we chosen a starting point in the inner region, convergence would have been immediate.

This is the big downside of a gradient-based algorithm: because it extrapolates local behavior across the entire curve it can massively overshoot. If this goes into a region where the function is not defined then it is hard to recover from that. Also there are configurations like the one that we've seen above that lead to infinite cycles around the root – and unfortunately those are not that rare. It turns out that in our specific problem, market scenarios with multiple levered curves regularly lead to such situations.

D.2.2 Introducing the learning rate η

We have seen above that in many instances the Newton-Raphson method can overshoot the root because it extrapolates local behavior across the entire curve. This problem can be mitigated by introducing a learning rate $\eta < 1$ that reduces the step size of the update, allowing the algorithm to adapt to change in the local conditions. This flexibility however comes at a cost in that the convergence of the algorithm in the quasi linear case is now slower.

To give an example, we consider the function $f(x) = mx + b$ at the point $x = x^{(0)}$. Standard Newton-Raphson would converge in a single step to the root $x^{(1)} = -b/m$. If we introduce a learning rate η the update rule becomes instead

$$x^{(s+1)} = x^{(s)} + \eta(x^{(s)} - x^{(\infty)}) \tag{D.5}$$

where $x^{(\infty)} = -b/m$ is the actual root of the function. In other words, like Zeno's arrow, at every step we get closer to the root by a constant percentage. However, unlike in

Zeno’s paradox, every step is constant time so for $\eta < 1$ the algorithm will indeed never quite reach the target.

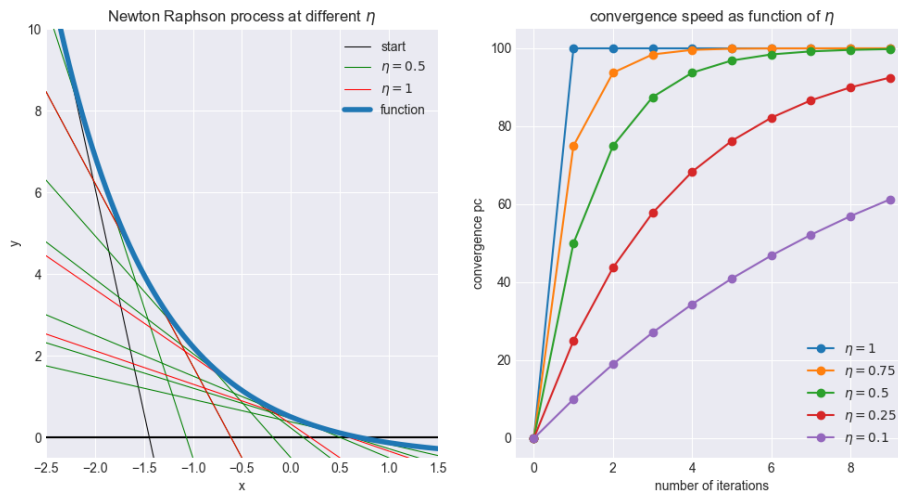


Figure D.6: *Impact of the learning rate on the Newton Raphson algorithm.* The left panel shows the mechanics of the Newton Raphson algorithm with learning rate $\eta = 1$ (red) and $\eta = 0.5$ (green), in line with the depiction in figure D.4 but with the labels (a), (b) omitted. The black line represents the first tangent. The red lines place the points (a) directly above the intersection and continue from there. The green lines only move the fraction η of the distance and place their new points (a) there. The right panel shows the convergence of the algorithm on a linear function. For $\eta = 1$ convergence is immediate, and for lower values of η it takes increasingly more steps to approach the target value which is never reached.

In figure D.6 we provided some analysis and illustration on the impact of the parameter η . In the left hand panel we are looking at the “Zeno convergence”, indicating how fast a linear function converges to the actual value. As we can see – at $\eta = 1$ convergence is perfect in step 1, but for any $\eta < 1$ convergence is slower and always asymptotic. On the right hand panel we visualized how a non-linear function converges according to different values of η : the red one is $\eta = 1$ and in this case convergence is very quick. The green one is $\eta = 0.5$, and here it takes significantly more steps to converge.

D.2.3 Higher dimensions

This algorithm easily generalizes to higher dimensions, where the gradient is replaced by the Jacobian matrix, and the tangent line by the tangent space. In the simple implementation shown above, effectively the function is replaced by its best linear approximation, and the root of that approximation is found. This “linear root” is then used to start the next step of the process.

More formally, if we have a function $f : \mathbb{R}^n \rightarrow \mathbb{R}^n$, the Jacobian matrix J at the point $\hat{\mathbf{x}} = (\hat{x}_1, \dots, \hat{x}_n)$ is defined as

$$J_{ij}(\hat{\mathbf{x}}) = \frac{\partial f_i}{\partial x_j}(\hat{\mathbf{x}}) \quad (\text{D.6})$$

and the linear approximation of the function f around $\hat{\mathbf{x}}$ is

$$f(\mathbf{x}) \simeq f(\hat{\mathbf{x}}) + J(\hat{\mathbf{x}}) \cdot (\mathbf{x} - \hat{\mathbf{x}}) \quad (\text{D.7})$$

The root of this linear approximation can be found by setting the right hand side to $\mathbf{0}$ and solving for \mathbf{x} . Specifically, if at step s we are at the point $\hat{\mathbf{x}}^{(s)}$ then, using the linear approximation for $\hat{\mathbf{x}}^{(s+1)}$, we get

$$\hat{\mathbf{x}}^{(s+1)} = \hat{\mathbf{x}}^{(s)} - J^{-1}(\hat{\mathbf{x}}^{(s)}) \cdot f(\hat{\mathbf{x}}^{(s)}) \quad (\text{D.8})$$

where $J^{-1}(\hat{\mathbf{x}}^{(s)})$ is the inverse of the Jacobian matrix at the point $\hat{\mathbf{x}}^{(s)}$.

Introducing the learning rate η we get the update rule⁴⁹

$$\hat{\mathbf{x}}^{(s+1)} = \hat{\mathbf{x}}^{(s)} + \Delta \hat{\mathbf{x}}^{(s)} \quad (\text{D.9})$$

⁴⁹In practice we use an update rule that first tries to invert the Jacobian, and if it is singular it uses another algorithm that inverts it only on its range, and does not attempt inversion on its null space

where

$$\Delta \hat{\mathbf{x}}^{(s)} = -\eta J^{-1}(\hat{\mathbf{x}}^{(s)}) \cdot f(\hat{\mathbf{x}}^{(s)}) \quad (\text{D.10})$$

E Explanation of key charts and tables

E.1 Curve charts

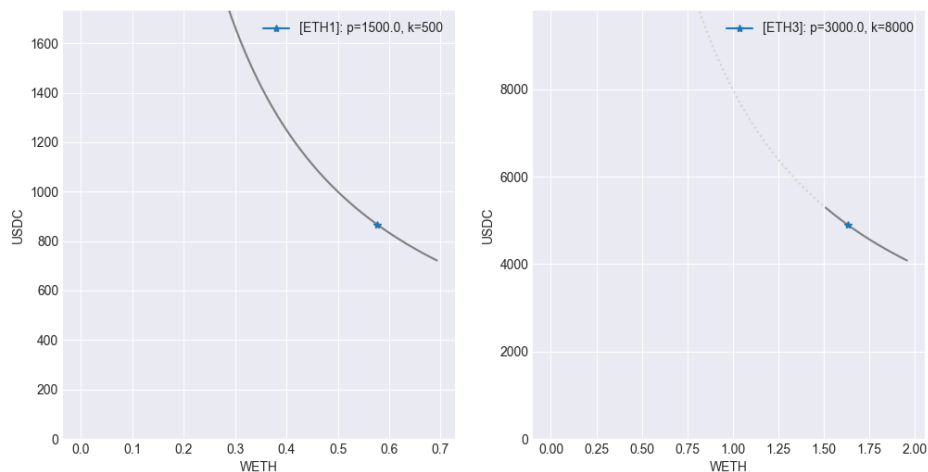


Figure E.1: *Representation of a single AMM curve with state.* The left panel shows an unlevered invariance (bonding) curve on the WETH/USDC pair: the AMM is indifferent between all combinations of token holdings on this curve, and currently it is at the point indicated by the star. The right hand curve shows a levered curve where the interpretation is the same, except that the state cannot go beyond the solid part of the curve. The dotted part is the associated unlevered curve.

Our key means of representing the state of the world are the *curve charts*. Fundamentally, they represent the invariance curves of the respective AMMs, with the current position marked with a star. We consider two types of curves, *levered* and *unlevered* ones. In the former, for example described by the traditional AMM equation 1.3, liquidity is placed all along the curve that therefore covers the entire price range between $p = 0$ and $p = \infty$. Such a curve is shown in the left hand panel of figure E.1. A levered curve on the other hand only places liquidity inside a certain price range, and the mechanism operates with virtual token balances as described in equation 1.5. Such a curve is shown in the right hand panel of figure E.1 where liquidity is only available for virtual ETH balances between roughly 1...2 WETH and 400...700 USDC. In both cases, the current state of the AMM on the curve is depicted by a star. Ignoring fees, all trades must happen

on the solid part of the respective curve. The dotted part on the right hand panel is only for information purposes – this is where the AMM would trade if the curve was unlevered with the same virtual token balances.

Here, both curves are trading WETH against USDC. The left, unlevered one has a pool constant $k = 500$, and the current price is $p = 1500$ USDC per WETH⁵⁰. The current state, as indicated by the blue star, is at virtual balances of 0.58 WETH and 866 USDC, the ratio of the two numbers corresponding to the price of 1500. This curve trades over the entire price range. The right hand curve is a levered curve that only trades in the small area where the curve is solid. The current price, again indicated by the blue star, is 3000, and the range is determined by the both ends of the solid curve at prices of 2,000 and 3500 respectively.

E.2 Trade instruction tables

In section 2.2 we have run the convex optimization algorithm on a number of curves, notably figure 2.1 (pair), figure 2.2 (triangle), figure 2.3 (triangle and pairs), and figure 2.4 (levered pair).

In table 2.1 (corresponding to figure 2.1) we see the trade instruction table associated with the pair trade. It contains the following lines:

- **Price line:** the post trade price of the respective token, in units of the “*target token*” in which the profit is taken (which can in this line be identified by a value of 1).
- **Curve lines** (*ETH1-3*): the trading lines corresponding to specific curves, as seen from the AMM. A negative number is an outflow of the respective token, and a positive number an inflow.
- **Aggregate lines** (*AMMIn*, *AMMOut*): aggregates all curves (“the AMM”, as opposed to “the trader”), separating (positive) inflows and (negative) outflows.

⁵⁰The price is always quoted as dy per dx

- **Net line:** the difference between aggregate in and outflows; in an arbitrage transaction all flows but one should be approximately zero, meaning that, in aggregate, no token flows happen in those tokens, and one flow (the one in the target token) should be negative, indicating the profit taken by the trader.

In table 2.2 (corresponding to figure 2.2) we are looking at a *triangle arbitrage*, meaning that we have three tokens (WETH, WBTC and USDC) and one curve each for the corresponding pairs. The structure of the table is the same as in table 2.1 except that we have one additional token column. In table 2.3 (corresponding to figure 2.3) finally we have 3 tokens and 3 curves per token, so a total of 9 curve lines.

F Implementation example

In this appendix we describe in more detail the assumptions made and data used in section 4. We have 7 tokens, TKN0 to TKN6, and their *base prices* (ie the prices they would have without deviations) are given in table F.1. For simplicity they follow a geometric progression. For example, TKN4 has twice the price of TKN3, and four times that of TKN2.

	TKN0	TKN1	TKN2	TKN3	TKN4	TKN5	TKN6
USD price	1	2	4	8	16	32	64

Table F.1: Token base prices

In the mostly-no-arbitrage case, corresponding to the curves in F.2, we have 17 curves C00 to C16 that exhibit prices close to their base price. There are also curves Ca0 to Ca2 which have a higher capacity and will be the main route for taking the arbitrage that we will consider by adding the curve in table F.3. However, those three curves on their own do not provide an arbitrage opportunity, as the prices are very close to the base prices.

We can confirm that there is only a very small arbitrage in the original scenario corresponding to table F.2 when we look at the trade instructions in table F.4 and F.5. The total arbitrage is about 400 USD, both when extracted via TKN0, and via TKN2.

When we add the curve CaX from table F.3 as shown in tables F.6 and F.7. However, that arbitrage massively increases to an amount of about 40,000 USD. This is unsurprising, given that the price of this curve is 20% off the base price, and the capacity the curve is 10 times bigger than that of the standard curves, and commensurate with the curves Ca0 to Ca2 that close the arbitrage⁵¹. As expected, most of the trading activity happens in those four curves and their associated tokens TKN1 to TKN4, plus TKN0 if the profit is taken in that token.

⁵¹Curve CaX trades TKN1 and TKN4, and the three other curves close this in a square via TKN2 and TKN3

cid	Pair	Price	Base Price	Deviation	L	L_USD	
C00	TKN6/TKN3	8.1411		8	1.8%	46,341	1,048,576
C01	TKN6/TKN3	8.0320		8	0.4%	46,341	1,048,576
C02	TKN0/TKN2	0.2524		1/4	1.0%	524,288	1,048,576
C03	TKN4/TKN3	2.0448		2	2.2%	92,682	1,048,576
C04	TKN3/TKN2	2.0374		2	1.9%	185,364	1,048,576
C05	TKN3/TKN2	1.9805		2	-1.0%	185,364	1,048,576
C06	TKN4/TKN1	8.0760		8	1.0%	185,364	1,048,576
C07	TKN4/TKN1	7.9879		8	-0.2%	185,364	1,048,576
C08	TKN2/TKN1	1.9979		2	-0.1%	370,728	1,048,576
C09	TKN6/TKN0	64.2628		64	0.4%	131,072	1,048,576
C10	TKN4/TKN2	4.0058		4	0.1%	131,072	1,048,576
C11	TKN4/TKN5	0.5073		1/2	1.5%	46,341	1,048,576
C12	TKN6/TKN4	4.0304		4	0.8%	32,768	1,048,576
C13	TKN1/TKN2	0.5006		1/2	0.1%	370,728	1,048,576
C14	TKN0/TKN5	0.0314		1/32	0.4%	185,364	1,048,576
C15	TKN0/TKN5	0.0314		1/32	0.3%	185,364	1,048,576
C16	TKN2/TKN3	0.5075		1/2	1.5%	185,364	1,048,576
Ca0	TKN1/TKN2	0.5000		1/2	-0.0%	2,621,440	7,414,552
Ca1	TKN2/TKN3	0.5000		1/2	0.0%	3,707,276	20,971,520
Ca2	TKN3/TKN4	0.5000		1/2	0.0%	3,707,276	41,943,040

Table F.2: Curve set with limited arbitrage opportunities

cid	Pair	Price	Base Price	Deviation	L	L_USD	
CaX	TKN1/TKN4	0.1500		1/8	20.0%	1,853,638	10,485,760

Table F.3: Additional curve providing arbitrage opportunity

It is important to understand that the trade instructions form a connected system that moves tokens around. Once those instructions are created, individual curves cannot simply be removed, even if their contribution to the arbitrage is minimal. Each curve plays a role, and if one is removed, the associated flows must be rerouted through other curves. This rerouting may or may not significantly increase costs, depending on the importance of the curve to a specific trade.

There is no straightforward way for us to determine which curves are important by simply examining the trade instruction table. The only reliable method we know is to rerun the optimization algorithm without certain curves and compare the results. For example in table F.8 we repeat the analysis from table F.6, but we remove the curve C00, which handled over 1,000 USD in trading volume. Despite this, the final profit is only reduced by 2 USD, or about 0.5 bp of the total profit. However, removing this curve causes significant rerouting through the other curves. The details of this rerouting are not immediately apparent from examining only the trade instructions tables (tables F.4, F.5, F.6, F.7, F.8, and the summary table F.9).

	TKN0	TKN1	TKN2	TKN3	TKN4	TKN5	TKN6
PRICE	1.00	1.99	3.99	7.97	15.96	31.74	64.38
C00				-536			66
C01				353			-44
C02	3,190		-803				
C03				-1,401	693		
C04			-2,405	1,191			
C05			1,315	-661			
C06		-2,105			262		
C07		777			-97		
C08		352	-176				
C09	979						-15
C10			-39		10		
C11					284	-143	
C12					29		-7
C13		400	-200				
C14	-1,990					63	
C15	-2,565					81	
C16			1,968	-991			
Ca0		575	-288				
Ca1			628	-314			
Ca2				2,360	-1,179		
AMMIn	4,169	2,105	3,911	3,904	1,276	143	66
AMMOut	-4,555	-2,105	-3,911	-3,904	-1,276	-143	-66
TOTAL NET	-386	0	0	0	0	0	0

Table F.4: Trade instructions with little arbitrage

	TKN0	TKN1	TKN2	TKN3	TKN4	TKN5	TKN6
PRICE	0.25	0.50	1.00	2.00	4.00	7.96	16.15
C00				-541			67
C01				348			-43
C02	3,355		-844				
C03				-1,402	693		
C04			-2,407	1,192			
C05			1,313	-660			
C06		-2,109			262		
C07		773			-97		
C08		353	-177				
C09	1,097						-17
C10			-42		11		
C11					277	-140	
C12					26		-7
C13		401	-201				
C14	-1,939					61	
C15	-2,513					79	
C16			1,966	-990			
Ca0		582	-291				
Ca1			586	-293			
Ca2				2,346	-1,173		
AMMIn	4,452	2,109	3,865	3,886	1,269	140	67
AMMOut	-4,452	-2,109	-3,962	-3,886	-1,269	-140	-67
TOTAL NET	-0	-0	-97	-0	-0	-0	-0

Table F.5: Trade instructions with little arbitrage, extracting via TKN2

	TKN0	TKN1	TKN2	TKN3	TKN4	TKN5	TKN6
PRICE	1.00	2.10	3.94	7.69	15.18	31.21	62.44
C00				-165			20
C01				724			-90
C02	-2,985		756				
C03				-2,321	1,155		
C04			-5,581	2,798			
C05			-1,860	946			
C06		-28,135			3,680		
C07		-25,254			3,322		
C08		-15,990	8,255				
C09	-14,978						236
C10			-5,034		1,281		
C11					1,393	-692	
C12					680		-167
C13		-15,942	8,231				
C14	-10,626					337	
C15	-11,200					355	
C16			-1,208	616			
Ca0		-114,981	59,331				
Ca1			-62,890	31,827			
Ca2				-34,425	17,326		
CaX		200,302			-28,838		
AMMIn	0	200,302	76,573	36,911	28,838	692	257
AMMOut	-39,789	-200,302	-76,573	-36,911	-28,838	-692	-257
TOTAL NET	-39,789	-0	-0	-0	-0	-0	-0

Table F.6: Trade instructions with arbitrage curve

	TKN0	TKN1	TKN2	TKN3	TKN4	TKN5	TKN6
PRICE	0.25	0.53	1.00	1.95	3.85	7.75	15.71
C00				-692			85
C01				197			-24
C02	14,145		-3,523				
C03				-2,348	1,169		
C04			-5,763	2,891			
C05			-2,042	1,039			
C06		-28,331			3,707		
C07		-25,450			3,349		
C08		-15,731	8,117				
C09	-2,863						45
C10			-5,266		1,342		
C11					709	-356	
C12					429		-106
C13		-15,683	8,093				
C14	-5,354					169	
C15	-5,928					187	
C16			-1,389	709			
Ca0		-113,146	58,354				
Ca1			-66,520	33,687			
Ca2				-35,484	17,863		
CaX		198,340			-28,567		
AMMIn	14,145	198,340	74,564	38,524	28,567	356	130
AMMOut	-14,145	-198,340	-84,503	-38,524	-28,567	-356	-130
TOTAL NET	-0	-0	-9,939	-0	-0	-0	-0

Table F.7: Trade instructions with arbitrage curve, extracting via TKN2

	TKN0	TKN1	TKN2	TKN3	TKN4	TKN5	TKN6
PRICE	1.00	2.10	3.94	7.69	15.18	31.22	62.41
C01				660			-82
C02	-2,798		708				
C03				-2,323	1,156		
C04			-5,579	2,797			
C05			-1,858	945			
C06		-28,136			3,681		
C07		-25,255			3,322		
C08		-15,989	8,255				
C09	-15,282						241
C10			-5,035		1,282		
C11					1,385	-688	
C12					649		-160
C13		-15,941	8,231				
C14	-10,566					335	
C15	-11,141					353	
C16			-1,205	615			
Ca0		-114,972	59,326				
Ca1			-62,842	31,802			
Ca2				-34,496	17,362		
CaX		200,293			-28,837		
AMMIn	0	200,293	76,519	36,819	28,837	688	241
AMMOut	-39,787	-200,293	-76,519	-36,819	-28,837	-688	-241
TOTAL NET	-39,787	0	0	0	0	0	0

Table F.8: Trade instructions with arbitrage curve, and removing C00

	TKN1	TKN2	TKN3	TKN4
PRICE	0.54	1.00	1.94	3.82
Ca0	-141,173	73,381		
Ca1		-80,385	40,818	
Ca2			-40,818	20,569
CaX	141,173			-20,569
AMMIn	141,173	73,381	40,818	20,569
AMMOut	-141,173	-80,385	-40,818	-20,569
TOTAL NET	0	-7,004	0	0

Table F.9: Trade instructions with arbitrage curves only